Dissociation of the nuclear basket triggers chromosome loss in aging yeast

Mihailo Mirkovic[1], Jordan McCarthy[1], Anne Cornelis Meinema[1], Julie Parenteau[2], Sung Sik Lee[1,3], Sherif Abou Elela[2], Yves Barral[1]

1-Institute of Biochemistry, Department of Biology, ETH Zürich, Zürich, Switzerland
2- Département de microbiologie et d'infectiologie, Faculté de médecine et des sciences de la santé, Université de Sherbrooke, Sherbrooke, QC, Canada
3-Scientific Center for Optical and Electron Microscopy, ETH Zürich, Switzerland

ABSTRACT:

In many organisms, aging is a clear risk factor for increased rates of chromosome mis-segregation, the main source of aneuploidy. Here, we report that old yeast mother cells lose chromosomes by partitioning them asymmetrically to their daughter cells together with the pre-existing (old) Sindle Pole Body (centrosome equivalent in yeast). Strikingly, remodelling of the NPC and the displacement of its nuclear basket triggered these asymmetric segregation events. Concomitantly, basket displacement also caused unspliced pre-mRNAs to leak to the cytoplasm. We show that removing the introns of three genes involved in chromosome segregation was sufficient to fully suppress chromosome loss in old cells. Furthermore, promoting pre-mRNA leakage in young cells also caused asymmetric chromosome partition and loss through the same three introns. Therefore, we propose that basket displacement from NPCs and its ensuing effects on pre-mRNA quality control are a key trigger of aging phenotypes such as aneuploidy.

INTRODUCTION

Cellular aging results in several conserved phenotypes, including chromosome mis-segregation, fragmentation of mitochondria, accumulation of damaged or misfolded proteins, and alteration of nuclear morphology[1-3]. Strikingly, in organisms as distinct as fungi, worms and mammals[4-6] aging also correlates with remodelling of the Nuclear Pore Complex (NPC), a ~50 MDa gateway that controls mRNA export and the nucleo/cytoplasmic distribution of proteins [7]. At least in dividing cells and upon expression of the progeriatric variant of Lamin A, progerin, the most prominent change observed on NPC is the loss of their nuclear basket[8,9]. This structure is formed by the protein TPR on the nucleoplasmic side of the NPC and acts in processes as diverse as mRNA export, the retention of pre-mRNAs in the nucleus, protein quality control and gene regulation [10-15]. The central position of the NPC in eukaryotic information flow and the broad range of function assumed by its basket suggests that altering their function could have very diverse effects on cell function. However, despite this and the fact that the reorganization of NPC architecture with age is prominent in a wide range of organisms, we know little about whether and how NPC remodelling contributes to aging.

The unicellular fungus *Saccharomyces cerevisiae*, a budding yeast, is a remarkably useful system for studying the role of NPCs in cellular aging [1,3]. Indeed, budding yeast undergoes replicative aging, causing the mother cell to bud off a limited number of daughter cells until it starts slowing down its division rate, enter senescence and die[16]. Importantly, several studies have emphasized that the yeast

38 NPC is remodelled during replicative aging[4,17,18], but the exact consequences of its reorganization are
39 not fully understood.

40 A prominent driver of replicative aging in budding yeast is the accumulation of extrachromosomal DNA
41 circles (also called eccDNAs) in the mother cell nucleus [19-21]. These DNA circles form during the cell's
42 lifetime through excision of genomic segments, generally by recombination between repeated
43 sequences [22]. The vast majority of these circles (>99%) stems from the rDNA locus and are referred to
44 as extrachromosomal rDNA circles (ERCs)[19]. As the cell age, these circles accumulate exponentially
45 through their replication in S-phase and their retention in the mother cell at mitosis[19,23]. By the end of
46 their life, yeast cells contain about 1000 ERCs, which represents roughly the same amount of DNA as
47 the rest of the genome[23]. Importantly, their retention in the mother cell relies on their anchorage to NPCs
48 via the megadalton protein complex called the SAGA complex [4,24]. These NPC-ERC units are then
49 confined to the mother part of the dividing nucleus by a lateral diffusion barrier forming in the nuclear
50 envelope in the future plane of cleavage [24-26]. Indeed, yeast cells undergo a closed mitosis, i.e., they do
51 not undergo nuclear envelope breakdown (NEBD). Remarkably, anchorage of ERCs to NPCs results in
52 the dissociation of their nuclear basket due to SAGA acetylating nucleoporins such as Nup60 on the
53 nuclear side of the NPC [24]. Consequently, a majority of the NPCs of old yeast cells lack a basket[4].
54 However, it is unknown whether this has consequences for the physiology and survival of the cell and
55 contributes to the aging process.

56 One way to approach the question of whether displacement of the basket from the NPCs contributes to
57 the aging process is to determine whether other aging phenotypes depend on basket displacement and
58 if so, how. Here we focused on chromosome instability in old yeast cells. In many metazoans, including
59 humans, aging results in increasing rates of chromosome mis-segregation and aneuploidy, correlating
60 with increasing prevalence of cancer [27,28]. Our understanding of the molecular mechanisms of
61 chromosome segregation errors in old cells remains rudimentary. Here, we report evidence that NPC
62 remodelling during yeast aging leads to chromosome loss from old mother cells and investigate the
63 underlying mechanisms.

64 **RESULTS**

65 **Aging yeast cells lose chromosomes**

66 To examine whether aging affects the karyotype of yeast cells, we visualized and followed the fate of
67 individual chromosomes in replicatively aging mother cells, using either TetO-labelled chromosome II or
68 chromosome IV as reporters. Chromosome IV is the second longest chromosome, while chromosome
69 II is of average size. Both chromosomes are labelled through inserting an array of 256 TetO repeats in
70 the vicinity of their centromere[29,30]. These chromosomes were visualized by expressing fluorescently
71 tagged versions of the TetR protein (TetR-GFP or TetR-mCherry; Figures 1A-B). We then monitored
72 them throughout the entire replicative lifespan of yeast mother cells trapped under the microscope using
73 a microfluidics platform [4,31]. The replicative age of each mother cell was measured by counting the
74 number of daughters that it budded off over time, defining how many budding events they have already
75 completed at a given time point (completed budding events, CBE). Bud size and the number and position

76 of the spindle pole bodies (SPBs/Centrosome equivalent, labelled with mCherry) were used to identify
77 the cell cycle stages at which the cells were imaged (Figure 1A).

78 Analysis of these images showed that all young mother cells (~0-3 CBE; t=0h) and their daughters
79 contained a fluorescent dot, documenting the presence of the labelled chromosomes in all of them.
80 However, when reaching the age of 18 to 22 CBE (t=24h), 10-15% of these now old mother cells had
81 lost their dot (Figures 1B-C). This was observed irrespectively of which chromosome was labelled and
82 which fluorescent tag was used. Fluorescence of the labelled SPB was not affected, indicating that dot
83 loss was not caused by some instability of fluorophores in old cells. To test if the loss of these fluorescent
84 chromosomal foci was due to the loss of the TetO array specifically or of the entire chromosome, we
85 included a second label (an array of 256 repeats of the LacO sequence) in the middle of the long arm
86 of chromosome IV (Figure 1B) and asked whether the cells that lost the TetO array lost the LacO repeats
87 as well. Analysis of these images showed that 85% of the cells lacking the TetO array had indeed lost
88 the LacO array (50/59). Thus, these cells had probably lost the entire chromosome. Supporting this
89 notion, loss of the TetO array was fatal to the cells. Indeed, more than 99% (145/146 chromosome II
90 loss events) of the dot-less cells failed to divide further, as expected for a haploid cell losing an entire
91 chromosome. We concluded that much like many other organisms, yeast undergoes a burst of
92 chromosome instability when reaching an old age (Figures 1A, C).

93 In contrast to chromosomes, extra-chromosomal DNA circles accumulate in the yeast mother cell with
94 age rather than being lost [30,32]. Similarly, deleting the centromere from a chromosome causes the
95 retention of both sister chromatids in the mother cell [30]. Remarkably, inserting a centromeric sequence
96 (*CEN*) into a DNA circle, was sufficient to cause this mini-chromosome to be lost from aged mother cells
97 at a similar rate as that observed for full-size chromosomes (~20% of old cells; Figures 1B-C). To
98 exclude the possibility that the TetO array used to label them is the cause of chromosome and mini-
99 chromosome loss in aging, we also characterized the stability of a circular mini-chromosome expressing
100 short-lived GFP as a marker instead of TetO repeats. Scoring of the GFP signal demonstrated that old
101 mother cells lost these mini-chromosomes at essentially the same rate as they lose the TetO labelled
102 one (Figures 1B-C). Therefore, the presence of a centromere was necessary and sufficient for
103 chromosomes and mini chromosomes to be lost from aging mother cells. We concluded that
104 chromosome loss in old cells is driven by their centromere.

105 **Aged cells asymmetrically partition both sister chromatids to the bud**

106 Given the prominent role of the centromere in chromosome loss, we rationalized that the loss of
107 chromosomes in old mother cells could be due to mitotic mis-segregation events. To determine whether
108 it was the case, we next focused our analysis on the cells that were imaged during their mitosis in our
109 time-lapse recordings of aging cells (Figure 2A). Analysis of anaphases in old mother cells revealed a
110 striking increase in the rate of chromosome II, IV and minichromosome missegregation (Figure 2B). In
111 600 total anaphase events captured in our movies we found that 66 (11%) of them co-segregated the
112 labelled sister-chromatids to a single pole with, 54/66(82%) of the missegregation events resulting in
113 asymmetric partition of the chromatids to the bud of these old mother cells (Figure 2C). This was virtually
114 never observed in young cells (Figure 2A-C). Remarkably, the frequency of chromosome loss in the old

115 mother cells and of sister-chromatids segregating asymmetrically to the bud were in the same size order,
116 irrespective of whether chromosome II or chromosome IV was labelled. Therefore, chromosome loss
117 from old mother cells seems fully explained by a rise in sister-chromatid non-disjunction with age and
118 the resulting segregation of chromosomes asymmetrically to the bud. Thus, we examined the
119 mechanism behind this peculiar mode of directed chromosome mis-segregation.

120 In budding yeast, the pre-existing (old) SPB, i.e., the SPB that the cell inherited from the previous
121 mitosis, segregates to the bud in ~95% of mitoses, i.e., in a highly biased manner [33-35]. This can be
122 easily monitored when stable SPB components, such as the core SPB protein Spc42, are labelled with
123 mCherry, the maturation of which is relatively slow (~45 minutes half-time) relative to the duration of
124 yeast mitosis (~50 minutes from spindle assembly to completion of cytokinesis). Therefore, in cells
125 expressing Spc42-mCherry as a reporter, the old SPB (Figure 2A, red arrowhead) shines brighter than
126 the newly synthesized one. Given the convergent bias of SPB and sister-chromatid inheritance by the
127 bud of old cells, we asked whether in old mother cells it is the old SPB that drives the non-disjoining
128 sister-chromatids to the bud. In other words, we wondered whether the co-segregating sister-chromatids
129 attach to and co-segregate with the old SPB. To test this possibility, we examined the partition of the
130 labelled chromosomes relative to the old and new SPBs in old mother cells (t=24h, Figures 2D, E). In
131 about 10% of old cells, SPB inheritance is inverted, i.e., the old SPB mis-segregates to the mother cell
132 [33,34]. Analysis of these events indicated that the non-disjoining sister-chromatids followed the old SPB
133 to the mother cell in 80% of the cases instead of going to the bud (Figures 2D, E). We conclude that
134 chromosome loss in aging mother cells is due to preferential attachment of sister-chromatids to the old
135 SPB, which then partitions them asymmetrically to the bud.

136 In budding yeast, both sister chromatids initially attach in a syntelic manner to the old SPB upon
137 replication, as this SPB is the first to be available. These initial syntelic attachments are then dissolved
138 by the aurora B kinase to allow sister-chromatids to reorient and ultimately reach bi-orientation and
139 partition symmetrically in mitosis [36,37]. As a consequence, failure to correct initial attachments errors
140 causes sister-chromatids to co-segregate with the old SPB to the bud [38]. Therefore, we hypothesized
141 that the loss of chromosomes by mother cells to their daughters might be due to the error correction
142 pathway being impaired in old yeast cells. To test this idea, we analysed the effects of reducing
143 Ipl1/aurora B function during aging. Cells carrying the temperature sensitive *ipl1-321* mutant allele and
144 grown at a permissive temperature (27°C) showed no detectable chromosome loss at a young age
145 (Figure 2F). However, they started losing chromosomes prematurely during replicative aging (Figure
146 2F), resulting in a shortened lifespan (Sup Fig 1A). Strikingly, the chromosome loss rate of the old *ipl1-*
147 *321* mutant cells (t=24h) was undistinguishable from that of the wild type cells, indicating that the effects
148 of age and reducing Ipl1 activity were not additive (Figure 2F). This suggests that age and the *ipl1-321*
149 mutation affect the same pathway. We concluded that old cells lose chromosomes due to defects in the
150 pathway dedicated to correcting chromosome attachment errors.

151 **ERC accumulation drives chromosome loss in aging**

152 To identify mechanisms behind the deterioration of mitotic error correction with age, we investigated
153 whether chromosome loss is causally linked to other aging events, particularly to the displacement of

154 the basket from NPCs[4]. Given that basket displacement is triggered by accumulating ERCs and their
155 SAGA-dependent anchorage to NPCs[4,24,25], we first investigated whether ERC accumulation promotes
156 chromosome loss. Recruitment of the deacetylase Sir2 to rDNA repeats is one of the mechanisms by
157 which cells keep the rate of ERC formation low. Therefore, the *sir2*Δ mutant cells show an increased
158 rate of ERC formation, accumulate these circles quicker and prematurely compared to wild type cells,
159 and show a reduced longevity[19,39]. Supporting the notion that ERC accumulation might promote
160 chromosome loss, these mutant cells also showed a strong increase in chromosome loss, prematurely
161 in life (Figure 3A and Sup 2A). To test further whether ERC accumulation could promote chromosome
162 loss, we asked whether reducing the rate of ERC formation delays it. Recombination in the rDNA locus
163 and the consequent excision of ERCs is stimulated by the presence of a replication fork barrier between
164 rDNA units. While these barriers prevent the transcription machinery to collide with replication forks
165 coming from neighbouring rDNA units, the stalling forks are fragile, causing high rates of double strand
166 breaks. Therefore, removing these fork barriers, for example by inactivating the fork barrier protein Fob1,
167 drastically decreases the rate at which ERCs form and accumulate, stabilizes the nuclear baskets of
168 NPCs and prolongs the life span of the cells[4,40]. Thus, we asked whether inactivating Fob1 had any
169 effect on chromosome loss in old cells. Analysis of chromosome II presence in *fob1*Δ mutant cells
170 trapped in our microfluidics platform demonstrated that only very few of them had lost the TetO signal
171 even after dividing 18 times or more (t=24h; Figure 3A; Sup Fig 2A). We concluded from these data that
172 chromosome loss correlated remarkably well with ERC levels, suggesting that ERC accumulation and
173 hence, possibly the displacement of the basket from NPCs might promote chromosome loss. Further
174 supporting this notion, removal of the SAGA subunit Sgf73, which mediates ERC attachment to NPCs
175 and the subsequent displacement of their nuclear basket, phenocopied the effect of the *fob1*Δ
176 mutation[24]. Unlike the wild type cells, the *sgf73*Δ mutant cells failed to show any significant increase in
177 chromosome loss at any age (Figures 3A Sup Fig 2A). Thus, our data suggest that ERC formation and
178 anchorage to NPCs triggers chromosome loss in old yeast cells.

179 **Nuclear basket remodelling drives chromosome loss**

180 We reported that SAGA-dependent anchorage of ERCs to NPCs leads to the displacement of the NPCs'
181 nuclear basket[24]. To investigate whether basket displacement promotes chromosome loss in some
182 manner, we sought next to genetically destabilize the basket and determined whether this accelerated
183 aging and the concomitant rise of chromosome instability. To do this, we disrupted the *MLP1* gene,
184 encoding the major isoform of the core basket protein TPR in yeast, and monitored the effect of that
185 mutation on chromosome II stability in aging cells. In stark contrast to the *sgf73*Δ and *fob1*Δ single
186 mutant and the wild type cells, the *mlp1*Δ single mutant cells exhibited a rapid increase in their
187 chromosome loss as they aged, along with a shortened lifespan (Figures 3A-B Sup Fig 2A). Thus, our
188 data suggest that displacement of the basket from NPCs as the cells age promotes chromosome loss
189 through some yet unknown mechanism.

190 **Introns in genes of the aurora B pathway drive asymmetric chromosome partition in aging**

191 The displacement of the nuclear basket from NPCs upon ERC anchorage weakened the molecular
192 pathway that corrects chromosome attachment errors (Figure 3A). This in turn caused old mother cells

193 to lose chromosomes to their buds. We wondered about the molecular mechanism linking asymmetric
194 chromosome partition to basket displacement. The basket of the nuclear pore has been involved in
195 various processes, such as mRNA export [41], protein quality control [11], docking of environmentally
196 regulated genes to the nuclear periphery upon their induction [15], as well as the retention in the nucleus
197 of faulty mRNAs, such as unspliced pre-mRNAs [10,42], as well as docking Mad1 and Mad2, two key
198 components of the mitotic Spindle Assembly Checkpoint(SAC), to the NPC[43,44].

199 The SAC components Mad1 and Mad2 bind Mlp1 and Mlp2 as well as Nup60 at the basket of the NPC
200 [44]. However, basket dissociation, which delocalizes Mad1/2 from the nuclear periphery, does not appear
201 to interfere with their function [44]. Nevertheless, we investigated whether SAC dysfunction could account
202 for aging phenotypes caused by basket dissociation and for the premature aging phenotype of the *mlp1*Δ
203 mutant cells. Arguing against this hypothesis, the *mad1*Δ and *mad2*Δ single mutant cells exhibited no
204 change in replicative longevity compared to the wild type cells and did not phenocopy *mlp1*Δ mutant
205 cells (Sup Fig3A). Therefore, we searched for other mechanisms through which basket displacement
206 could trigger chromosome loss.

207 While perusing through the list of genes involved in chromosome segregation (Figure 4A) we noticed
208 that, surprisingly, only three of them contain an intron, namely *NBL1*, *MCM21* and *GLC7*. Strikingly,
209 these three genes function with Ipl1/aurora B in preventing syntelic chromosome attachment.
210 Nbl1/borealin is a component of the chromosome passenger complex of which aurora B/Ipl1 is the
211 catalytic subunit. Mcm21/CENP-O is a docking receptor for Ipl1/aurora B at kinetochores. Glc7/PP1A is
212 the protein phosphatase 1, which counteracts aurora B by dephosphorylating its targets at the outer-
213 kinetochore [45-47]. Intrigued by this remarkable convergence, we wondered whether asymmetric
214 chromosome partition in aging could stem from the presence of these three introns in error correction
215 genes. Indeed, we rationalized that displacement of the basket from NPCs could potentially affect the
216 regulation, export and hence expression of intron-containing transcripts, specifically, thereby affecting
217 the function of the *NBL1*, *MCM21* and *GLC7* genes.

218 To investigate the possibility that the introns of *GLC7, MCM21, NBL1* contribute to the rise of
219 chromosome loss in old cells, we removed them from each of the three genes (-*Δi* alleles) and imaged
220 the mutant cells throughout their replicative lifespan. Removing their introns individually or all three
221 simultaneously (*3xΔi* strain) had no detectable effects on chromosome segregation in young cells
222 (Figure 4B). In sharp contrast, simultaneously removing all three introns nearly completely suppressed
223 chromosome loss in old cells (Figure 4B-C). Removing them individually or in pair did so as well, albeit
224 the effects were milder. Removing the introns of the two α-tubulin genes *TUB1* and *TUB3* simultaneously
225 had no effect, indicating that the effects observed with the introns of *NBL1*, *MCM21* and *GLC7* were
226 specific (Figure 4B). The effects observed were similar for chromosome II and chromosome IV,
227 indicating that the role of these introns was not chromosome specific (Sup Figure 3B). Furthermore,
228 removing these three introns also suppressed the occurrence of asymmetric anaphases in old cells
229 (Figure 4C), supporting the view that asymmetric chromosome segregation and chromosome loss go
230 hand-in-hand and are under the control of these three introns. Strengthening this conclusion, removal
231 of these introns also suppressed chromosome loss in the *ipl1-321* mutant cells (Sup Figure 1B).

232 Remarkably, simultaneous removal of *MCM21*, *NBL1* and *GLC7* introns had also a substantial effect on
233 the longevity of the cells, extending their replicative lifespan up to ~20% (Figure 4D). A similar effect
234 was observed in the *ipl1-321* mutant cells (Sup Fig1 A). This suggests that chromosome loss is the first
235 direct cause of death for many yeast cells upon aging, although other mechanisms eventually take over
236 when chromosome loss is abrogated.

237 **Basket destabilization causes intron-dependent chromosome loss in young cells**

238 Thus, our data indicate that basket dissociation from NPCs promotes chromosome loss through an
239 intron-dependent dampening of the error correction pathway. To test this idea more in depth, we asked
240 whether mutations affecting the nuclear basket also promote chromosome loss outside of the aging
241 context. Thus, we characterized chromosome segregation in young *mlp1*Δ cells (Figure 5A-C). Analysis
242 of chromosome II segregation indicated that the *mlp1*Δ mutant cells not only exhibited a four-fold
243 increase in their chromosome mis-segregation rate compared to the young wild type cells, but ~80% of
244 these mis-segregation events followed the old SPB, as in old cells (Figure 5C). Furthermore, this effect
245 was suppressed upon removal of the introns of *MCM21*, *NBL1* and *GLC7*(Figure 5B). Therefore,
246 although to a lower extent than in old cells, defects of the nuclear basket result in asymmetric
247 chromosome partition also in young cells. Like in aging, these effects are mediated through the introns
248 of *MCM21*, *NBL1* and *GLC7.* Interestingly, while the lifespan of the *mlp1*Δ mutant cells was shortened
249 compared to wild type, removal of these three introns rescued chromosome loss and partially restored
250 the longevity of the cells (Figure 5D-E). We concluded that intron-dependent dampening of the error
251 correction pathway is one, even if not the only one, progeriatric effects of the *mlp1*Δ mutation. Possibly,
252 other introns contribute to other aging phenotypes. Thus, our data indicate that basket displacement
253 promotes chromosome loss in young mutant cells and old wild type mother cells.

254 **Old cells leak pre-mRNA to the cytoplasm**

255 Furthermore, our data suggested that the role of the nuclear basket in enforcing proper chromosome
256 segregation involved its function in mRNA processing and quality control, and particularly in some
257 process related to splicing or to intron function. Thus, to explore this possibility, we next investigated
258 whether old mother cells show defects in pre-mRNA quality control. Indeed, basket mutant cells fail to
259 retain unspliced pre-mRNAs in the nucleus [10,42]. We therefore reasoned that old yeast mother cells might
260 show similar defects.

261 As a first proof of principle, we went on to characterize the localization of intronic RNA sequences in
262 young and old cells, using single molecule RNA fluorescence in situ hybridization (smRNA FISH). For
263 these studies, we focused on three introns, namely those of the *DBP2*, *YRA1* and *GLC7* genes. Indeed,
264 most yeast introns are short (50-150 nucleotides) and well below the size detectable by smRNA FISH
265 (>500 nts, ideally >1 kb). In the yeast genome, only 20 introns are longer than the required minimal size.
266 Thus, we chose to develop probes for the long introns, namely those of *DBP2* (766 nts), and *YRA1*
267 (1002 nts), and for obvious reasons for *GLC7* (525 nts). The introns of *NBL1* (66 nts) and *MCM21* (88
268 nts) are too short for this method. Cohorts of old cells were collected using the Mother Enrichment
269 Program (MEP)[48] followed by FACS sorting to reach high homogeneity. By inducing cell death in the
270 daughter cells specifically, the MEP ensures that aging mother cells are diluted linearly instead of

271 exponentially in the population, greatly simplifying the isolation of very old cells. FACS sorting ensured
272 that the cohorts were free of young cells and young cell debris. With each of these three series of
273 smRNA FISH probes, we detected one or two nuclear foci in young cells. Only very rarely did we observe
274 a focus in the cytoplasm (<3% of the cells). No foci were detected in the corresponding *Δi* strains,
275 demonstrating probe specificity (Sup Fig4). In contrast, for each of the three introns tested, smRNA
276 FISH detected intronic RNA sequences in the cytoplasm of the majority of old cells. For example, in the
277 case of *GLC7,* ~70% of smRNA FISH foci were found in the cytoplasm of old mother cells, compared to
278 ~3% in young cells (Figures 6A-B Sup Fig4). Together, these data indicated that 3 of 3 tested introns
279 showed a strong tendency to leak to the cytoplasm in old mother cells. However, this first test did not
280 clarify whether the full pre-mRNA or only the intron escaped from the nucleus.

281 To address this question very directly, we turned to a functional assay and monitored the translation of
282 an unspliced pre-mRNA reporter in the cytoplasm. This fluorescent reporter construct expresses GFP
283 upon proper splicing of the nascent transcript, or mCherry, coded in the intron, when the unspliced pre-
284 mRNA leaks out of the nucleus and hence, becomes translated (Figure 6C) [49]. Cells carrying this
285 construct integrated at the *TRP1* locus were trapped and imaged in our microfluidics platform. The
286 fluorescence levels of the two reporter fluorophores as well as the number of completed budding events
287 of the recorded cells were measured as they aged. Analysis of the fluorescence signal established that
288 the mCherry/GFP ratio increased in old compared to young cells, demonstrating elevated translation of
289 the pre-mRNA in the cytoplasm of aged cells compared to young ones (Figures 6D-E).

290 Consistent with leakage and translation of this reporter depending on ERC accumulation, the
291 mCherry/GFP ratio increased prematurely and to a higher level in the *sir2*Δ mutant, compared to the
292 wild type cells. In reverse, the *fob1*Δ mutant cells showed a lowered mCherry/GFP ratio, which did not
293 increase much during their lifespan (Figures 6D-E). Thus, we conclude that ERC formation and
294 accumulation promotes pre-mRNA leakage during yeast aging, as expected from their effect on the
295 NPCs' nuclear basket.

296 **pre-mRNA leakage induces asymmetric chromosome partition**

297 Given the results above, we wondered whether chromosome loss in old cells is linked to their failure to
298 retain pre-mRNAs in the nucleus. Thus, we asked whether inducing pre-mRNA leakage would alone be
299 sufficient for triggering chromosome loss. The two yeast SR-protein Gbp2 and Hrb1 have been
300 implicated in the retention of pre-mRNAs in the nucleus by binding intron-containing transcripts and
301 delaying their export until they are properly spliced or degraded[50,51].Therefore*, hrb1*Δ *gbp2*Δ double
302 mutant cells leak pre-mRNA to the cytoplasm at a higher rate than wild type cells [10,50-52]. Thus, we asked
303 whether these double mutant cells showed any tendency to lose the labelled chromosome II. As a
304 control, we asked whether the *snu66*Δ mutation, which affects the spliceosome itself directly [53,54], lead
305 to similar phenotypes.

306 The young spliceosome-defective, *snu66*Δ mutant cells did exhibit a five-fold elevated level of
307 chromosome mis-segregation compared to young wild type cells. However, this mis-segregation was
308 not biased towards any specific SPB (Figures 7A-B), suggesting that it involved a distinct mechanism
309 than that observed in old cells and in young cells lacking the basket protein Mlp1. In contrast to the

310 *snu66*Δ mutant, the *hrb1*Δ *gbp2*Δ double mutant cells, showed an even stronger increase in their rate
311 of chromosome mis-segregation, which was more than ten-fold above that of young wild type cells.
312 Furthermore, sister-chromatid mis-segregation was strongly biased towards the old SPB. Removing the
313 introns of *GLC7, MCM21* and *NBL1* suppressed this chromosome segregation defect (Figure 7A).
314 Therefore, pre-mRNA leakage is sufficient to induce asymmetric chromosome partition and is contingent
315 on the presence of introns in the error correction genes *NBL1*, *MCM21* and *GLC7*. The fact that
316 mutations affecting the spliceosome did not cause such an asymmetric segregation of chromosome to
317 the bud indicates that the effects observed in old cells cannot be explained simply by splicing defects.

318 We conclude that the loss of the NPCs' basket and subsequent leakage of pre-mRNAs impairs the
319 correction of syntelic attachments by the Ipl1/aurora B pathway, resulting in asymmetric partition of
320 sister-chromatids and chromosome loss with age. Basket displacement and pre-mRNA leakage
321 inhibited error correction by some yet unknown mechanism involving the introns of the *NBL1*, *MCM21*
322 and *GLC7* genes, specifically.

323 **DISCUSSION**

324 Aging manifests itself through a broad diversity of conserved cellular phenotypes but except in few cases
325 we know little about how these relate or are causally linked to each other[1-3]. In this study we investigated
326 whether NPC remodelling in old mother cells contributes to the emergence of other aging phenotypes,
327 taking chromosome loss as a study case[4]. We show that NPC remodelling is both necessary and
328 sufficient for the raise of chromosome loss with age and provide insights into the mechanisms involved.
329 Indeed, interventions that promote displacement of the NPCs' basket and basket defects in general
330 promoted non-disjunction and mis-segregation of sister-chromatids to the bud, and hence chromosome
331 loss in the old mother cell. These interventions include mutations that stimulate ERC formation and
332 removal of the main yeast TPR isoform, Mlp1. In reverse, interventions that prevent NPC remodelling,
333 such as delaying ERC accumulation, their anchorage to NPCs and the recruitment of SAGA to NPCs,
334 restored proper chromosome segregation in old cells and prevented chromosome loss. Thus, NPC
335 remodelling appeared as the pivotal point for triggering chromosome loss in old cells.

336 Two potential caveats should be considered. First, the *sir2*Δ and *fob1*Δ mutations have each more
337 effects than only influencing ERC formation. The *sir2*Δ mutant cells lose silencing of the hidden mating
338 type loci, genetically behaving as diploids, fail to silence subtelomeric regions and act through some yet
339 unknown mechanism on the maintenance of proper proteostasis[55-58]. Likewise, the *fob1*Δ mutation
340 renders the rDNA locus unstable, which might interfere with rRNA transcription and ribosome
341 biosynthesis[59]. However, their only clear common denominator is that they both affect ERC formation,
342 and hence NPC remodelling even if in opposite manners[39,40]. Moreover, the *sgf73*Δ mutation
343 phenocopies the effects of the *fob1*Δ mutation. Here again the only known functional overlap between
344 Fob1 and Sgf73 resides in their requirements for the accumulation of ERCs in the mother cell, and
345 indirectly (Fob1) or directly (Sgf73), for their anchorage to NPCs and the consequent displacement of
346 NPCs' basket[4,24]. In fitting, the fact that destabilizing the basket also promotes the premature onset of
347 chromosome loss reinforces the notion that it is indeed the displacement of the basket from NPCs that
348 triggers chromosome loss upon ERC accumulation.

349 A second possible caveat is that chromosome loss could be linked to aging in some other manner. The
350 effects of the diverse perturbations listed above would promote chromosome loss indirectly, via the
351 effects that they have on cellular aging. To address this possibility, we investigated the molecular
352 mechanisms that link basket displacement and chromosome loss. Our data reveal that chromosome
353 loss is due to the non-correction of syntelic chromosome attachments in old cells. In young cells, such
354 corrections are enforced by the kinase aurora B and its accessory factors[36]. Our data also show that the
355 inhibition of correction in old cells requires the presence of three introns, those standing in the genes
356 *NBL1*, *MCM21* and *GLC7*. These three genes are the only genes of the chromosome segregation
357 machinery to have kept an intron. Strikingly, the proteins Nbl1, Mcm21 and Glc7 are all involved in the
358 error correction pathway, together with aurora B/Ipl1[45-47]. Removing their introns sufficed for restoring
359 proper attachment correction and chromosome segregation in old cells and for suppressing the
360 premature chromosome loss phenotype of the *ipl1-321* mutant cells grown at semi-permissive
361 temperature. Intron removal delays cell death but does not abrogate aging. Furthermore, the
362 suppression of chromosome mis-segregation upon removal of these introns is not only observed in old
363 wild type cells but also in young *mlp1*Δ mutant cells. Thus, intron removal separates aging and
364 chromosome loss, indicating that the action of these introns is part of the proximal cause of chromosome
365 loss and is independent of age. Therefore, our data indicate that there is a direct, intron-dependent link
366 between basket displacement from NPCs and chromosome loss. We suggest that this link relates to the
367 role of the nuclear basket of the NPC in inhibiting the export of unspliced pre-mRNAs out of the nucleus,
368 and hence, in mRNA quality control. The fact that another, independent set of mutations that also
369 interfere with pre-mRNA retention in the nucleus, such as the *gbp2*Δ *hrb1*Δ double mutant cells, also
370 increase the rate of chromosome loss through the same three introns strengthens this conclusion. Thus,
371 together our data establish that displacement of the nuclear basket from NPCs in old mother cell triggers
372 chromosome non-disjunction and loss.

373 This conclusion has several consequences and opens new questions. The key question stems from our
374 observation that releasing pre-mRNA from the nucleus relaxes the control that cells impose on
375 chromosome attachment. The question is, how does this work? Does it involve the translation of the
376 pre-mRNAs in the cytoplasm? Does it come about through the correlated loss of properly mature
377 mRNAs and hence, the reduced expression of their products? Two arguments speak against these
378 interpretations. First, if any of these two options were to account for the effect of pre-mRNA leakage,
379 mutations affecting splicing efficiency would lead to the same effects. However, tempering with the
380 spliceosome does not affect the correction of chromosome attachment errors to any extent and
381 specificity close to the effects of pre-mRNA leakage. Second, since Mcm21 and Glc7 have opposite
382 effects on chromosome correction it is unclear how impairing the expression of both would lead to the
383 synergistic effects that we observe between them. Finally, analysis of RNA-seq data from replicatively
384 aged cells indicate that if aging indeed impairs the splicing of some transcripts, such as those encoding
385 ribosomal proteins, it stimulates that of others[60]. This suggests that aging has a non-univocal effect on
386 intron-containing transcripts. It will be important to determine whether basket displacement contributes
387 to these effects, how it does so and whether this could explain the effect it has on the error correction
388 pathway.

389 Our observations that basket displacement has such profound and highly specific impacts on processes
390 functionally very distant from that of the NPC, such as chromosome segregation, has several
391 consequences. First, it means that NPC remodelling could affect many more cellular functions than only
392 chromosome segregation. Interestingly, beyond mRNA quality control the basket of the NPC is also
393 involved in protein quality control and the activation of environmentally regulated genes, two processes
394 that are indeed impaired in old cells[1,2]. Thus, basket displacement might contribute to these phenotypes
395 in aging cells. It is also very tempting to speculate that the role of the basket in mRNA quality control
396 could affect more than only chromosome segregation. Indeed, while budding yeasts have kept only a
397 subset of the introns of their ancestors, these introns are not distributed randomly and seem to be
398 enriched in very suggestive genes, such as genes coding for ubiquitin-conjugating enzymes and
399 proteasome subunits, components of the mitochondrial respiratory chain and ribosomal proteins[61].
400 Since decay of the ubiquitin-mediated protein degradation, mitochondrial membrane potential and
401 function and of ribosome assembly are classical and ubiquitous hallmarks of aging[1-3], it is possible that
402 basket displacement in old cells contributes to the emergence of these aging phenotypes as well.

403 A second type of consequences emerging from our observations stems from the fact that displacement
404 of the NPCs' basket is also observed in stressed cells and not solely in the context of aging. For example,
405 heat shock also causes basket displacement in yeast[62]. Therefore, it is possible that the downstream
406 effects we observe in old cells also take place during stress response. In this respect, it is interesting to
407 note that heat shock has been associated with a strong raise in aneuploidy in yeast[63-65]. Furthermore,
408 aneuploidy is a frequent response to environmental stresses and a primary mechanism for the
409 emergence of stress resistant clones in fungi[66]. Therefore, it is tempting to speculate that the
410 chromosome mis-segregation resulting from basket displacement might be a selected response to
411 stress. It might indeed be selectively advantageous for cells to have means to promote karyotype
412 variations when their survival is in question. It is therefore worth considering that a similar process,
413 perhaps using similar mechanisms, underlies the aneuploidy of cancer cells.

414 Third, the role of basket displacement in the emergence of aging phenotypes is likely not a peculiarity
415 of yeast. Using proteomics, basket displacement has been inferred to take place in aging cells such as
416 the hepatocytes of old mice and humans[6,67]. Little is known about whether the nuclear basket plays any
417 similar role in pre-mRNA retention in the nucleus of metazoans as of yeast cells, but it is still striking that
418 intron-retention is one of the hallmarks of aging on the metazoan transcriptome, and that pre-mRNA
419 processing genes are important in mitotic stability[68-71]. Such intron-retention would be expected if some
420 transcripts tend to escape the nucleus prematurely. More striking maybe, the perhaps most ubiquitous
421 effect of the expression of the progeriatric variant of lamin A, progerin, across cell types is the
422 displacement of the nuclear basket protein TPR from NPCs[8]. We know still very little about the impact
423 of basket displacement in the etiology of the Gilford-Hutchinson Progeria Syndrome, but our yeast
424 studies suggest that it might be relevant. If so, investigating the potential effects of progerin on pre-
425 mRNA leakage might become an essential step towards understanding and perhaps mitigating the
426 effects of progerin expression.

427 In a broader sense, our findings might bring fundamental insights towards our understanding of aging.
428 For decades, the role of ERCs in aging has been perceived as a yeast peculiarity. However, the effect

429 it has on NPCs may close the gap. On one hand, it seems to illuminate what might be the commonality
430 between ERC-driven aging in yeast and other aging processes in other eukaryotes. Indeed, the basket-
431 centric view of aging that we propose here would explain how ERCs actually cause aging in yeast and
432 indicate that while ERC accumulation might be an idiosyncrasy of yeast, the downstream events are
433 not. On the other hand, this idea open two corollary questions. 1) What is the biological significance of
434 eccDNAs promoting basket displacement in yeast? 2) What causes basket displacement in other aging
435 systems. We are intrigued by the idea that ERCs and any replicating eccDNA for that matter are the
436 closest mimics that laboratory yeast strain may encounter of pathogenic DNA of exogenous origin. In
437 that perspective, basket displacement and the ensuing effects might have first appeared as a response
438 to infections. In other words, yeast aging might reflect the activity of a death pathway that normally
439 functions in pathogen control. It might represent some fungal version of what an auto-inflammatory or
440 auto-immune response in metazoans would be. Therefore, it will be interesting to investigate whether
441 exogenous or non-chromosomal DNA, such as possibly that of viruses, also triggers the displacement
442 of the nuclear basket from NPCs in yeast and other systems, and whether this contributes to either or
443 both of anti-viral defence and aging. If so, aging might have emerged as an anti-viral defence.

444 **Author Contributions:**
445 Conceptualization: MM, ACM, YB Investigation: MM, JM, ACM Formal Analysis: MM,JM, ACM,CD
446 Writing-original draft: YB,MM Writing – review & editing: MM,JM,JP,SAE,YB Resources: JP,SSL
447 Supervision: YB Funding acquisition: YB

448 **Acknowledgments:**
449 We acknowledge Dr.Dan Jarosz, Dr. Gabriel Neurohr, Dr. Madhav Jagannathan, Dr. Patrick Meraldi
450 ,Dr Anna Marzelliusardottir for critical reading and suggestions on the Manuscript. We acknowledge
451 the ScopeM facility at the Institute of Biochemistry, ETH for their technical assistance. We
452 acknowledge Elisa Dultz for providing the Chromosome II strain with the POA1::TetO array.

453 **Funding:**
454 MM: grant 31003A-105904 from the Swiss National Science Foundation (SNSF) and the ETH
455 postdoctoral fellowship 19-1 FEL-10

456 JM: grant 31003A-105904 from the Swiss National Science Foundation (SNSF)

457 JP: CIHR (Canadian institute of health research) 201809PJT-407549-BMB-CFDA-53473.

458 SSL: Scope M facility of ETH Zurich, Institute of Biochemistry

459 SAE: CIHR (Canadian institute of health research) 201809PJT-407549-BMB-CFDA-53473.

460 YB: grant 31003A-105904 from the Swiss National Science Foundation (SNSF)

461 **Declaration of interests:**
462 Authors declare that they have no competing interests.

463 **Data and materials availability:**
464 All the raw data generated in the manuscript will be deposited in the Mendelay online repository.

465

466 **Main Figure Legends**

467 **Figure 1 Old cells lose chromosomes**
468 **A)** Cells carrying labeled Chromosome II and imaged at different ages on the microfluidic chip. Time of
469 acquisition is indicated on the left. Fluorescent markers are indicated on top. Replicative age of imaged
470 cells (completed budding event – CBE) is indicated in merged images. Scale bar (upper right panel) is
471 5µm. Green arrow marks the TetR-GFP foci **B)** Schematic representation of the chromosome labels
472 used in this study. **C)** Chromosome loss fraction of indicated chromosomes after 0h (~0-3 CBE) and
473 24h (~18-22 CBE) of imaging. The mode of chromosome visualization is indicated in parenthesis, i.e.,
474 TetR-GFP (green), TetR-mCherry (red) or mini-chromosome encoded GFP (GFP exp). Chromosome
475 loss is defined as the absence of the label in the mother cell in G1 shortly after the final cell cycle, or the
476 final anaphase. Each data point represents a fraction of chromosome loss in a cohort of ~50 cells.
477 Unpaired T-test (*<0.05, **<0.005, ***<0.0005).
478

479 **Figure 2 Old cells lose chromosome by asymmetric sister chromatid partition**
480 **A)** Images of anaphase cells carrying the labeled chromosome II as in Fig. 1A. Red arrows mark the old
481 SPBs. **B)** Fraction of anaphase mis-segregation events where chromosomes are visible only in the
482 mother or daughter cell (n>150) Bars are labelled as in Fig 1C. Each data point represents frequency of
483 anaphase missegregation in the cohort of ~50 anaphases **C**) Fraction of anaphase missegregation
484 events that lead to TetR-GFP foci being present in the mother or the daughter cell (n=66, cohorts of 10).
485 **D)** Graphical schematic of all observed anaphase missegregation events and their frequency. **E)**
486 Fraction of anaphase mis-segregation events biased towards the old (red) or new SPB (pink) for mini-
487 chromosome (n=30) and Chr II with normal (Daughter(D)) and inverted segregation of the old SPB
488 (Mother (M)) (n=60 and 30). Cohorts of 10-20 missegregating anaphases **F)** Fraction of Chromosome
489 II loss in *wt*, *lpl1-321*, at 0h (~0-3 CBE), 12h (~8-12 CBE) and 24h (~18-22 CBE) at 27°C. Each data
490 point represents loss frequency in a cohort of ~50 cells. Unpaired T-test (*<0.05, **<0.005, ***<0.0005).
491

492 **Figure 3 ERC formation and NPC remodeling drive chromosome loss and aging**
493 **A)** Loss fraction of Chromosome II in strains of indicated genotype as a function of CBE (divided into
494 categories of 5xCBE)*(N, n(cells/divisions) wt=458/8600, sir2Δ=158/1779, fob1Δ=127/2681,*
495 *sgf73Δ=142/3950 mlp1Δ=302/4270)* **B)** Replicative lifespan of listed genotypes (n>120 cells , Log-rank
496 (Mentel Cox) test *<0.05,**<0.005,***<0.0005).

497 **Figure 4 Introns drive asymmetric chromatid partition and chromosome loss in aging**
498 **A)** A list of genes encoding kinetochore-associated proteins. Adapted from Biggins et al 2013. Intron
499 containing genes are marked in red. **B)** Fraction of Chromosome II loss at indicated aging time (top) in
500 cells of indicated genotype. *3xΔi stands for GLC7-Δi MCM21-Δi NBL1-Δi* triple mutant. Each data point
501 represents a fraction of chromosome loss in a cohort of ~50 cells. Unpaired T-test (*<0.05, **<0.005,
502 ***<0.0005). **C)** Fraction of anaphase missegregation of Chromosome II at indicated aging time (top) in
503 cells of indicated genotype. *3xΔi stands for GLC7-Δi MCM21-Δi NBL1-ΔI* triple mutant. Each data point
504 represents missegregation frequency in a cohort of ~50 anaphases. Unpaired T-test (*<0.05, **<0.005,
505 ***<0.0005). **D)** Replicative lifespan upon intron removal (n>200 cells, Log-rank (Mentel Cox) test,
506 *<0.05, **<0.005, ***<0.0005).

507 **Figure 5 Basket displacement causes intron-dependent chromosome loss in young and old cells**
508 **A)** Stills of symmetric and asymmetric anaphases in young cells. Arrow marks the old SPB. Scale bar
509 (upper right panel) is 5µm **B)** Anaphase mis-segregation of Chromosome II in cells of indicated
510 genotypes *(n=2774,3000,2700).* Each data point represents anaphase missegregation fraction in the
511 cohort of >300 cells. **C)** Fraction of Chromosome II missegregation with old (red) or new SPB (pink) in
512 anaphase cells of indicated genotype (n=30 cohorts of ~10 missegregation events) Unpaired T-test
513 (*<0.05, **<0.005, ***<0.0005) **D)** Chromosome II loss probability in indicated genotype as a function of
514 CBE (divided into categories of 5xCBE) *(N, n(cells/divisions) wt=458/8600, mlp1Δ=302/4270, mlp1Δ*
515 *3xΔi=295/4757)* **E)**Replicative lifespan of listed genotypes. Red and green stars represent *p-values*
516 between the wt and the corresponding genotype. Black stars represent the p-value between *mlp1Δ* and
517 *mlp1Δ 3xΔi* (n>300 cells, Log-rank (Mentel Cox) test, *<0.05, **<0.005, ***<0.0005).

518

Figure 6 Pre-mRNA leaks to the cytoplasm in aging
A) Images of RNA FISH targeting three long introns (*GLC7, YRA1, DBP2*) in young and old cells. **B)** Quantification of *GLC7* intron RNA FISH foci localization in young and old cells (n=295, cohorts of ~100 cells) **C)** Principle of the pre-mRNA translation reporter (left panel) adapted from (*Sorenson et al. 2014*). **D)** Images of the pre-mRNA translation reporter in cells (right panel) of indicated genotype (top) at indicated ages (bottom). **E)** Log2 ratio of mCherry/GFP in cells of indicated genotype as a function of age, normalized to wt median at 0h (n=60, 35, 32). Unpaired T-test comparing the log2 ratio of mCherry/GFP intensity of cells at 12 or 24h (*<0.05, **<0.005, ***<0.0005).

Figure 7 Pre-mRNA leakage is sufficient to drive asymmetric chromatid partition
A) Anaphase mis-segregation of Chromosome II in cells of indicated genotypes *(n=2774,5269,2650,1607).* Each data point represents anaphase missegregation fraction in the cohort of >300 cells **B)** Fraction of Chromosome II missegregation with old (red) or new SPB (pink) in anaphase cells of indicated genotype (n=50,30 cohorts of ~10 missegregation events). Unpaired T-test (*<0.05, **<0.005, ***<0.0005).

Supplementary Figure Legends

Figure S1 Introns inhibit mitotic error correction in aging
A) Replicative lifespan of wt, GLC7Δi, Ipl1-321 and Ipl1-321 GLC7Δi cells grown at 27 Celsius (n=300), Log-rank (Mentel Cox) test *<0.05,**<0.005,***<0.0005.**B)** Fraction of Chromosome II loss in wt, *Ipl1-321*, *Ipl1-321 3xΔi (GLC7-Δi MCM21-Δi NBL1Δi)* at 0h (~0-3 CBE), 12h (~8-12 CBE) and 24h (~18-22 CBE) at 27°C. Each data point represents loss frequency in a cohort of ~50 cells**.** Unpaired T-test (*<0.05, **<0.005).

Figure S2 Chromosome loss in aging is ERC and NPC remodeling dependent
A) Fraction of Chromosome II loss (*POA1:TetO* /TetR-GFP) in wt, *fob1*Δ,*sir2*Δ, sgf73Δ and *mlp1*Δ mutant cells at 0h (~0-3 CBE),12h (~8-12 CBE) and 24h (~18-22 CBE). Each data point represents a fraction of loss in a cohort of ~50 cells. Stars correspond to *p-values* of wt vs genotype of listed color at the corresponding timepoint. Unpaired T-test (*<0.05, **<0.005, ***<0.0005).

Figure S3 The effect of introns on chromosome loss is not chromosome-specific
A) Replicative lifespan of *wt, mad1*Δ, *mad2*Δ cells. n>100 cells, Log-rank (Mentel Cox) test. **B)** Fraction of Chromosome II, IV and GFP minichromosome loss (See Fig 1B) upon removal of intron of *GLC7* 0h (~0-3 CBE) and 24h (~18-22 CBE). Each data point represents a fraction of loss in a cohort of ~50 cells. Unpaired T-test (*<0.05, **<0.005, ***<0.0005).

Figure S4 smRNA FISH probes are intron specific
A) Images of smRNA FISH experiments in wt and *GLC7-Δi* cells B) Quantification of smRNA FISH foci per cell in wt and *GLC7-Δi* cells C) Quantification of smRNA FISH foci per cell in wt cells at 0 and 28h of aging (n>300, cohorts of 100+ cells)

Materials and methods

Lead contact

Further information and requests for resources and reagents should be directed to and will be fulfilled by the Lead Contact, Yves Barral (yves.barral@bc.biol.ethz.ch).

Materials availability

This study generated ~50 novel yeast strains, derived either by crossing or transformation. All strains are available to the public upon request

Experimental Model Details

Strains and plasmids

All yeast strains and plasmids used in this study are listed in the **Supplementary file1**. Strains are derived from S288C background. For every strain derived from a cross, an appropriate control strain was always selected from the same tetrad. Protein C-terminal yeGFP-tag and knock-out strains were

570 generated using methods described in *Janke et al 2004* [72]. All cultures were grown using standard
571 conditions at 160 rpm, in YPD or synthetic drop-out medium supplemented with 0.1% BSA for aging
572 chips (SD-medium; ForMedium, Norfolk, UK) at 25°C or 30°C.

573 **Intron-less strains**
574
575 Intron deletions were conducted in two independent colonies of the strain JPY10I, as outlined previously
576 in Parenteau *et al* 2008 [73]. Briefly, each intron was individually deleted using a modified two-step process
577 (pop-in / pop-out), ensuring the absence of any additional sequence or markers post-deletion. The
578 deletions were done in diploid strains, confirmed via PCR, and three distinct haploid strains bearing the
579 confirmed deletions were chosen for subsequent analyses. Combinations of different Δ-intron strains
580 have been derived by crossing and validated by PCR for the absence of the intron.
581
582 **Chromosome and Plasmid reporter strains**
583
584 Multiple chromosomes and minichromosome visualization strains have been used in this study: **1)**
585 Chromosome II reporter strain, with the centromere proximal TetO array (*POA1* locus) strain was kindly
586 provided by Elisa Dultz from the Weis Lab, ETH, institute of Biochemistry (internal reference KWY3759).
587 **2)** Chromosome IV TetO (Centromere proximal) and LacO (centromere distal) were acquired from
588 strains used in *Neurohr et al 2011* [29], originally derived from *Vas AC et al 2006* [74] **3)** Ubi-GFP
589 minichromosome (PYB 2665) was derived by cloning UBIYdkGFP* from *Houser et al 2012* (PNC 1136)
590 [75] into a PYB 2640 backbone by homologous recombination in yeast. **4)** A minichromosome reporter
591 containing the TetO array was previously described in *Denoth-Lippuner et al 2014* [24].

592 **Materials and methods**
593
594 **Microscopy**

595 For confocal fluorescent microscopy, yeast cells were precultured in YPD, and then washed in synthetic
596 drop-out medium. One ml of cells from exponential growing cultures with OD <1 was concentrated by
597 centrifugation at 1500 rcf, washed in SD complete, and resuspended in ~10 µl of low fluorescent SD-
598 medium, spotted on a round coverslip and immobilized with a SD/agar patch. The cells were imaged in
599 >15 z-stacks slices with 0.3 µm spacing, with a 100×/1.4 NA objective on a DeltaVision microscope
600 (Applied Precision) equipped with a CCD HQ2 camera (Roper), 250 W Xenon lamps, Softworx software
601 (Applied Precision) and a temperature chamber set to 30°C.
602
603 **Aging microfluidic platform**

604 Chromosome segregation and protein intensity during aging were assessed using the high-throughput
605 yeast aging analysis (HYAA) microfluidics dissection platform [31]. The PDMS (polydimethylsiloxane)
606 microchannel is made by soft-lithography and bonded on the 30 mm micro-well cover glass in the 55
607 mm glass bottom dish (Cellvis, CA, USA). For the lifespan analyses, a chip with a new cell trapping
608 design was used [4], to ensure excellent retention of old cells.

609 To start the aging experiment, yeast cells were pre-cultured for 24 hr in SD-full media supplemented
610 with 0.1% Albumin Bovine Serum (protease free BSA; Acros Organics, Geel, Belgium). Young cells from
611 an exponentially growing culture were captured in the traps of the microfluidic chip; the chip was
612 continuously flushed with fresh medium at a constant flow of 10 µl/min, using a Harvard PHD Ultra
613 syringe pump (Harvard Apparatus, Holiston, MA, USA) with 60 ml syringe per lane, with inner diameter
614 26.7 mm (Becton Dickinson, Franklin Lakes, NJ, USA). Bright field images in a single z focal plane were
615 recorded every 15 min throughout the duration of the entire experiment to measure replicative age of
616 cells. To record fluorescent signals, images with a florescent lamp and at least 13x z-stacks (0.5 µm
617 step) were acquired in 12h intervals. For imaging we used an epi-fluorescent microscope (TiE, Nikon
618 Instruments, Tokyo, Japan) controlled by Micro-Manager 1.4.23 software [76], with a Plan Apo 60 × 1.4
619 NA objective. For fluorescence illumination of the GFP and mCherry labelled proteins, a Lumencor
620 Spectra-X LED Light Engine was used. Z stacks of >13 slices with 0.5 µm spacing were recorded for
621 fluorescent imaging every 12 hours in order to cover the entire volume of the nucleus during the aging
622 process. Transmitted light imaging was done in a single Z plane to minimize the light exposure of the

623 cells. The age of the cell was defined by the number of daughter cells that emerged during the budding
624 cycles (CBE).

625 **Chromosome loss assessment**

626 For the assessment of chromosome and mini-chromosome loss and mis-segregation in aging, trapped
627 cells in the chip that had the labeled chromosomes at the initial time point of 0h (~virtually all cells) were
628 followed in transmitted light channel and fluorescent images were acquired every 12 hours. Only cells
629 where the entire volume of the nucleus was in focus and imaged, and where SPB was clearly visible
630 were considered in the analysis. The background fluorescence was subtracted in FIJI using a subtract
631 background function. The aged nuclei were examined by scrolling through the z stack (>13 stacks,
632 0,5um step) in both channels, to validate the presence of the SPBs and TetR foci in the mother or the
633 daughter cell. "Chromosome loss" refers to two quantified events: 1) The absence of the chromosome
634 from a mother or a daughter cell compartment during anaphase 2) A G1 mother cell that just underwent
635 its final division and is clearly viable, with a present SPB dot, but no chromosome dot. When
636 "Chromosome loss" is listed, it pertains to the sum of these two events. When "chromosome loss in
637 anaphase" is listed, it only pertains to the loss frequency observed during anaphase. Cells which lost
638 chromosomes due to abnormal mitotic events in the last replicative division, such as SPB
639 overamplification or full nuclei migration into the bud (Combined ~10% of all cells in the final replicative
640 division) were discarded from the quantifications. All cells were examined in the DIC channel for signs
641 of disrupted morphology indicating cell death and followed up in DIC to confirm cell death after
642 chromosome loss. For the assessment of minichromosome loss in aging (TetO array or ubi-GFP
643 minichromosome) the yeast cultures were grown in SD-LEU or SD-URA selective media enabling
644 minichromosome maintenance in all starting young cells. When loaded onto an aging chip cell were
645 transferred to SD complete media, allowing them to lose the minichromosome during aging without
646 inducing cell death. As the cells were grown in selective media, the minichromosome loss rate at 0h is
647 N/A. In general, aging chips are not suitable for measurement of chromosome loss rate in young cells,
648 as cells within the young population that are missegregating chromosomes are usually stressed and
649 enlarged, and thus cannot be loaded into the microfluidic traps intended for the normal young cells. For
650 chromosome missegregation rates in young cells, we have used classical confocal imaging on a patch
651 of SD agar, as described in the Microscopy section.

652 **Measurements of chromosome loss per CBE**
653
654 To measure chromosome loss probability per Completed Budding Event (CBE), we utilized at least 150
655 cells per genotype and quantified the number of cells that lost the reporter chromosome during a specific
656 replicative division. The number of losses at a specific CBE was then divided by total number of cells
657 which passed though mitosis at that CBE number to give the probability of chromosome loss per CBE.
658 Categories of 5x CBE and its mean value of chromosome loss were plotted along with its SD.
659
660 **Mother Enrichment Program (MEP) with FACS and RNA FISH**
661
662 Mother Enrichment Program was performed according to the standard procedure, using the strains
663 acquired from the Gotchling Lab [48]. Cells were labeled with Biotin and aged for 28h, after which they
664 were fixed in 4% PFA for 30 minutes. The cells were then stained with streptavidin conjugated with a
665 FACS compatible fluorophore (647nm) and sorted using FACSAria III at the Flow Cytometry Core
666 Facility at ETH Zurich to enrich for old mother cells. After FACS sorting, single molecule RNA FISH with
667 Stellaris® probes designed for introns of *GLC7, YRA1, DBP2* was performed as described in *Rahman*
668 *et al 2013* [77].
669
670 **Quantification and Statistical analysis.**
671
672 Statistical analyses were performed using GraphPad Prism 10 software

673

674

675

676 **Resources table**

REAGENT or RESOURCE	SOURCE	Reference
Critical commercial assays		
GEL extraction	QIAGEN	Ref:28604
Plasmid extraction	MACHEREY-NAGEL	Ref:740588.250
Experimental models: Organisms/strains		
Full strain list	Mihailo Mirkovic	Supp file 1
Primers	Mihailo Mirkovic	See Supp file 1
smRNA FISH probes	Biosearch Technologies	See Supp file 1
Recombinant DNA		
CEN TetO-plasmid	*Dennoth-L et al 2014*	YYB 16094
Ubi-GFP plasmid	This study	PYB 2665
Software and algorithms		
Graphpad Prism	Dotmatics	
ImageJ-FIJI		
Microsoft Excel	Microsoft	
Microsoft Word	Microsoft	
Adobe Illustrator	Adobe	

677

678 **References**

679 1. Denoth Lippuner, A., Julou, T., and Barral, Y. (2014). Budding yeast as a model organism to study the
680 effects of age. FEMS Microbiol Rev *38*, 300-325. 10.1111/1574-6976.12060.
681 2. Lopez-Otin, C., Blasco, M.A., Partridge, L., Serrano, M., and Kroemer, G. (2023). Hallmarks of aging: An
682 expanding universe. Cell *186*, 243-278. 10.1016/j.cell.2022.11.001.
683 3. Janssens, G.E., and Veenhoff, L.M. (2016). Evidence for the hallmarks of human aging in replicatively
684 aging yeast. Microb Cell *3*, 263-274. 10.15698/mic2016.07.510.
685 4. Meinema, A.C., Marzelliusardottir, A., Mirkovic, M., Aspert, T., Lee, S.S., Charvin, G., and Barral, Y.
686 (2022). DNA circles promote yeast ageing in part through stimulating the reorganization of nuclear pore
687 complexes. Elife *11*. 10.7554/eLife.71196.
688 5. D'Angelo, M.A., Raices, M., Panowski, S.H., and Hetzer, M.W. (2009). Age-dependent deterioration of
689 nuclear pore complexes causes a loss of nuclear integrity in postmitotic cells. Cell *136*, 284-295.
690 10.1016/j.cell.2008.11.037.
691 6. Ori, A., Toyama, B.H., Harris, M.S., Bock, T., Iskar, M., Bork, P., Ingolia, N.T., Hetzer, M.W., and Beck,
692 M. (2015). Integrated Transcriptome and Proteome Analyses Reveal Organ-Specific Proteome
693 Deterioration in Old Rats. Cell Syst *1*, 224-237. 10.1016/j.cels.2015.08.012.
694 7. Dultz, E., Wojtynek, M., Medalia, O., and Onischenko, E. (2022). The Nuclear Pore Complex: Birth, Life,
695 and Death of a Cellular Behemoth. Cells *11*. 10.3390/cells11091456.
696 8. Larrieu, D., Vire, E., Robson, S., Breusegem, S.Y., Kouzarides, T., and Jackson, S.P. (2018). Inhibition
697 of the acetyltransferase NAT10 normalizes progeric and aging cells by rebalancing the Transportin-1
698 nuclear import pathway. Sci Signal *11*. 10.1126/scisignal.aar5401.
699 9. Merideth, M.A., Gordon, L.B., Clauss, S., Sachdev, V., Smith, A.C., Perry, M.B., Brewer, C.C., Zalewski,
700 C., Kim, H.J., Solomon, B., et al. (2008). Phenotype and course of Hutchinson-Gilford progeria
701 syndrome. N Engl J Med *358*, 592-604. 10.1056/NEJMoa0706898.
702 10. Galy, V., Gadal, O., Fromont-Racine, M., Romano, A., Jacquier, A., and Nehrbass, U. (2004). Nuclear
703 retention of unspliced mRNAs in yeast is mediated by perinuclear Mlp1. Cell *116*, 63-73. 10.1016/s0092-
704 8674(03)01026-2.
705 11. Niepel, M., Molloy, K.R., Williams, R., Farr, J.C., Meinema, A.C., Vecchietti, N., Cristea, I.M., Chait, B.T.,
706 Rout, M.P., and Strambio-De-Castillia, C. (2013). The nuclear basket proteins Mlp1p and Mlp2p are part
707 of a dynamic interactome including Esc1p and the proteasome. Mol Biol Cell *24*, 3920-3938.
708 10.1091/mbc.E13-07-0412.

709 12. Saroufim, M.A., Bensidoun, P., Raymond, P., Rahman, S., Krause, M.R., Oeffinger, M., and Zenklusen,
710 D. (2015). The nuclear basket mediates perinuclear mRNA scanning in budding yeast. J Cell Biol *211*,
711 1131-1140. 10.1083/jcb.201503070.
712 13. Albert, S., Schaffer, M., Beck, F., Mosalaganti, S., Asano, S., Thomas, H.F., Plitzko, J.M., Beck, M.,
713 Baumeister, W., and Engel, B.D. (2017). Proteasomes tether to two distinct sites at the nuclear pore
714 complex. Proc Natl Acad Sci U S A *114*, 13726-13731. 10.1073/pnas.1716305114.
715 14. Aksenova, V., Smith, A., Lee, H., Bhat, P., Esnault, C., Chen, S., Iben, J., Kaufhold, R., Yau, K.C.,
716 Echeverria, C., et al. (2020). Nucleoporin TPR is an integral component of the TREX-2 mRNA export
717 pathway. Nat Commun *11*, 4577. 10.1038/s41467-020-18266-2.
718 15. Raices, M., and D'Angelo, M.A. (2017). Nuclear pore complexes and regulation of gene expression. Curr
719 Opin Cell Biol *46*, 26-32. 10.1016/j.ceb.2016.12.006.
720 16. Mortimer, R.K., and Johnston, J.R. (1959). Life span of individual yeast cells. Nature *183*, 1751-1752.
721 10.1038/1831751a0.
722 17. Rempel, I.L., Steen, A., and Veenhoff, L.M. (2020). Poor old pores-The challenge of making and
723 maintaining nuclear pore complexes in aging. FEBS J *287*, 1058-1075. 10.1111/febs.15205.
724 18. Rempel, I.L., Crane, M.M., Thaller, D.J., Mishra, A., Jansen, D.P., Janssens, G., Popken, P., Aksit, A.,
725 Kaeberlein, M., van der Giessen, E., et al. (2019). Age-dependent deterioration of nuclear pore
726 assembly in mitotic cells decreases transport dynamics. Elife *8*. 10.7554/eLife.48186.
727 19. Sinclair, D.A., and Guarente, L. (1997). Extrachromosomal rDNA circles--a cause of aging in yeast. Cell
728 *91*, 1033-1042. 10.1016/s0092-8674(00)80493-6.
729 20. Jin, M., Li, Y., O'Laughlin, R., Bittihn, P., Pillus, L., Tsimring, L.S., Hasty, J., and Hao, N. (2019).
730 Divergent Aging of Isogenic Yeast Cells Revealed through Single-Cell Phenotypic Dynamics. Cell Syst
731 *8*, 242-253 e243. 10.1016/j.cels.2019.02.002.
732 21. Morlot, S., Song, J., Leger-Silvestre, I., Matifas, A., Gadal, O., and Charvin, G. (2019). Excessive rDNA
733 Transcription Drives the Disruption in Nuclear Homeostasis during Entry into Senescence in Budding
734 Yeast. Cell Rep *28*, 408-422 e404. 10.1016/j.celrep.2019.06.032.
735 22. Moller, H.D., Mohiyuddin, M., Prada-Luengo, I., Sailani, M.R., Halling, J.F., Plomgaard, P., Maretty, L.,
736 Hansen, A.J., Snyder, M.P., Pilegaard, H., et al. (2018). Circular DNA elements of chromosomal origin
737 are common in healthy human somatic tissue. Nat Commun *9*, 1069. 10.1038/s41467-018-03369-8.
738 23. Bitterman, K.J., Medvedik, O., and Sinclair, D.A. (2003). Longevity regulation in Saccharomyces
739 cerevisiae: linking metabolism, genome stability, and heterochromatin. Microbiol Mol Biol Rev *67*, 376-
740 399, table of contents. 10.1128/MMBR.67.3.376-399.2003.
741 24. Denoth-Lippuner, A., Krzyzanowski, M.K., Stober, C., and Barral, Y. (2014). Role of SAGA in the
742 asymmetric segregation of DNA circles during yeast ageing. Elife *3*. 10.7554/eLife.03790.
743 25. Shcheprova, Z., Baldi, S., Frei, S.B., Gonnet, G., and Barral, Y. (2008). A mechanism for asymmetric
744 segregation of age during yeast budding. Nature *454*, 728-734. 10.1038/nature07212.
745 26. Baldi, S., Bolognesi, A., Meinema, A.C., and Barral, Y. (2017). Heat stress promotes longevity in
746 budding yeast by relaxing the confinement of age-promoting factors in the mother cell. Elife *6*.
747 10.7554/eLife.28329.
748 27. Boveri, T. (2008). Concerning the origin of malignant tumours by Theodor Boveri. Translated and
749 annotated by Henry Harris. J Cell Sci *121 Suppl 1*, 1-84. 10.1242/jcs.025742.
750 28. Jacobs, P.A., Court Brown, W.M., and Doll, R. (1961). Distribution of human chromosome counts in
751 relation to age. Nature *191*, 1178-1180. 10.1038/1911178a0.
752 29. Neurohr, G., Naegeli, A., Titos, I., Theler, D., Greber, B., Diez, J., Gabaldon, T., Mendoza, M., and
753 Barral, Y. (2011). A midzone-based ruler adjusts chromosome compaction to anaphase spindle length.
754 Science *332*, 465-468. 10.1126/science.1201578.
755 30. Kruitwagen, T., Chymkowitch, P., Denoth-Lippuner, A., Enserink, J., and Barral, Y. (2018). Centromeres
756 License the Mitotic Condensation of Yeast Chromosome Arms. Cell *175*, 780-795 e715.
757 10.1016/j.cell.2018.09.012.
758 31. Jo, M.C., Liu, W., Gu, L., Dang, W., and Qin, L. (2015). High-throughput analysis of yeast replicative
759 aging using a microfluidic system. Proc Natl Acad Sci U S A *112*, 9364-9369.
760 10.1073/pnas.1510328112.
761 32. Gehlen, L.R., Nagai, S., Shimada, K., Meister, P., Taddei, A., and Gasser, S.M. (2011). Nuclear
762 geometry and rapid mitosis ensure asymmetric episome segregation in yeast. Curr Biol *21*, 25-33.
763 10.1016/j.cub.2010.12.016.

764 33. Lengefeld, J., Hotz, M., Rollins, M., Baetz, K., and Barral, Y. (2017). Budding yeast Wee1 distinguishes
765 spindle pole bodies to guide their pattern of age-dependent segregation. Nat Cell Biol *19*, 941-951.
766 10.1038/ncb3576.
767 34. Pereira, G., Tanaka, T.U., Nasmyth, K., and Schiebel, E. (2001). Modes of spindle pole body inheritance
768 and segregation of the Bfa1p-Bub2p checkpoint protein complex. EMBO J *20*, 6359-6370.
769 10.1093/emboj/20.22.6359.
770 35. Hotz, M., Leisner, C., Chen, D., Manatschal, C., Wegleiter, T., Ouellet, J., Lindstrom, D., Gottschling,
771 D.E., Vogel, J., and Barral, Y. (2012). Spindle pole bodies exploit the mitotic exit network in metaphase
772 to drive their age-dependent segregation. Cell *148*, 958-972. 10.1016/j.cell.2012.01.041.
773 36. Biggins, S., Severin, F.F., Bhalla, N., Sassoon, I., Hyman, A.A., and Murray, A.W. (1999). The
774 conserved protein kinase Ipl1 regulates microtubule binding to kinetochores in budding yeast. Genes
775 Dev *13*, 532-544. 10.1101/gad.13.5.532.
776 37. Cheeseman, I.M., Anderson, S., Jwa, M., Green, E.M., Kang, J., Yates, J.R., 3rd, Chan, C.S., Drubin,
777 D.G., and Barnes, G. (2002). Phospho-regulation of kinetochore-microtubule attachments by the Aurora
778 kinase Ipl1p. Cell *111*, 163-172. 10.1016/s0092-8674(02)00973-x.
779 38. Tanaka, T.U., Rachidi, N., Janke, C., Pereira, G., Galova, M., Schiebel, E., Stark, M.J., and Nasmyth, K.
780 (2002). Evidence that the Ipl1-Sli15 (Aurora kinase-INCENP) complex promotes chromosome bi-
781 orientation by altering kinetochore-spindle pole connections. Cell *108*, 317-329. 10.1016/s0092-
782 8674(02)00633-5.
783 39. Kaeberlein, M., McVey, M., and Guarente, L. (1999). The SIR2/3/4 complex and SIR2 alone promote
784 longevity in Saccharomyces cerevisiae by two different mechanisms. Genes Dev *13*, 2570-2580.
785 10.1101/gad.13.19.2570.
786 40. Defossez, P.A., Prusty, R., Kaeberlein, M., Lin, S.J., Ferrigno, P., Silver, P.A., Keil, R.L., and Guarente,
787 L. (1999). Elimination of replication block protein Fob1 extends the life span of yeast mother cells. Mol
788 Cell *3*, 447-455. 10.1016/s1097-2765(00)80472-4.
789 41. De Magistris, P. (2021). The Great Escape: mRNA Export through the Nuclear Pore Complex. Int J Mol
790 Sci *22*. 10.3390/ijms222111767.
791 42. Bonnet, A., and Palancade, B. (2015). Intron or no intron: a matter for nuclear pore complexes. Nucleus
792 *6*, 455-461. 10.1080/19491034.2015.1116660.
793 43. Iouk, T., Kerscher, O., Scott, R.J., Basrai, M.A., and Wozniak, R.W. (2002). The yeast nuclear pore
794 complex functionally interacts with components of the spindle assembly checkpoint. J Cell Biol *159*, 807-
795 819. 10.1083/jcb.200205068.
796 44. Scott, R.J., Lusk, C.P., Dilworth, D.J., Aitchison, J.D., and Wozniak, R.W. (2005). Interactions between
797 Mad1p and the nuclear transport machinery in the yeast. Molecular Biology of the Cell *16*, 4362-4374.
798 10.1091/mbc.E05-01-0011.
799 45. Pinsky, B.A., Kotwaliwale, C.V., Tatsutani, S.Y., Breed, C.A., and Biggins, S. (2006). Glc7/protein
800 phosphatase 1 regulatory subunits can oppose the Ipl1/aurora protein kinase by redistributing Glc7. Mol
801 Cell Biol *26*, 2648-2660. 10.1128/MCB.26.7.2648-2660.2006.
802 46. Poddar, A., Roy, N., and Sinha, P. (1999). MCM21 and MCM22, two novel genes of the yeast
803 Saccharomyces cerevisiae are required for chromosome transmission. Mol Microbiol *31*, 349-360.
804 10.1046/j.1365-2958.1999.01179.x.
805 47. Nakajima, Y., Tyers, R.G., Wong, C.C., Yates, J.R., 3rd, Drubin, D.G., and Barnes, G. (2009). Nbl1p: a
806 Borealin/Dasra/CSC-1-like protein essential for Aurora/Ipl1 complex function and integrity in
807 Saccharomyces cerevisiae. Mol Biol Cell *20*, 1772-1784. 10.1091/mbc.e08-10-1011.
808 48. Lindstrom, D.L., and Gottschling, D.E. (2009). The mother enrichment program: a genetic system for
809 facile replicative life span analysis in Saccharomyces cerevisiae. Genetics *183*, 413-422, 411SI-413SI.
810 10.1534/genetics.109.106229.
811 49. Sorenson, M.R., and Stevens, S.W. (2014). Rapid identification of mRNA processing defects with a
812 novel single-cell yeast reporter. RNA *20*, 732-745. 10.1261/rna.042663.113.
813 50. Hackmann, A., Wu, H., Schneider, U.M., Meyer, K., Jung, K., and Krebber, H. (2014). Quality control of
814 spliced mRNAs requires the shuttling SR proteins Gbp2 and Hrb1. Nat Commun *5*, 3123.
815 10.1038/ncomms4123.
816 51. Hurt, E., Luo, M.J., Rother, S., Reed, R., and Strasser, K. (2004). Cotranscriptional recruitment of the
817 serine-arginine-rich (SR)-like proteins Gbp2 and Hrb1 to nascent mRNA via the TREX complex. Proc
818 Natl Acad Sci U S A *101*, 1858-1862. 10.1073/pnas.0308663100.

819 52. Windgassen, M., Sturm, D., Cajigas, I.J., Gonzalez, C.I., Seedorf, M., Bastians, H., and Krebber, H.
820 (2004). Yeast shuttling SR proteins Npl3p, Gbp2p, and Hrb1p are part of the translating mRNPs, and
821 Npl3p can function as a translational repressor. Mol Cell Biol *24*, 10479-10491.
822 10.1128/MCB.24.23.10479-10491.2004.
823 53. Stevens, S.W., and Abelson, J. (1999). Purification of the yeast U4/U6.U5 small nuclear
824 ribonucleoprotein particle and identification of its proteins. Proc Natl Acad Sci U S A *96*, 7226-7231.
825 10.1073/pnas.96.13.7226.
826 54. Murphy, M.W., Olson, B.L., and Siliciano, P.G. (2004). The yeast splicing factor Prp40p contains
827 functional leucine-rich nuclear export signals that are essential for splicing. Genetics *166*, 53-65.
828 10.1534/genetics.166.1.53.
829 55. Haber, J.E. (2012). Mating-type genes and MAT switching in Saccharomyces cerevisiae. Genetics *191*,
830 33-64. 10.1534/genetics.111.134577.
831 56. Rine, J., and Herskowitz, I. (1987). Four genes responsible for a position effect on expression from HML
832 and HMR in Saccharomyces cerevisiae. Genetics *116*, 9-22. 10.1093/genetics/116.1.9.
833 57. Gottschling, D.E., Aparicio, O.M., Billington, B.L., and Zakian, V.A. (1990). Position effect at S.
834 cerevisiae telomeres: reversible repression of Pol II transcription. Cell *63*, 751-762. 10.1016/0092-
835 8674(90)90141-z.
836 58. Smith, J.S., and Boeke, J.D. (1997). An unusual form of transcriptional silencing in yeast ribosomal
837 DNA. Genes Dev *11*, 241-254. 10.1101/gad.11.2.241.
838 59. Kobayashi, T., Heck, D.J., Nomura, M., and Horiuchi, T. (1998). Expansion and contraction of ribosomal
839 DNA repeats in Saccharomyces cerevisiae: requirement of replication fork blocking (Fob1) protein and
840 the role of RNA polymerase I. Genes Dev *12*, 3821-3830. 10.1101/gad.12.24.3821.
841 60. Gomez-Montalvo, J., de Obeso Fernandez Del Valle, A., De la Cruz Gutierrez, L.F., Gonzalez-Meljem,
842 J.M., and Scheckhuber, C.Q. (2024). Replicative aging in yeast involves dynamic intron retention
843 patterns associated with mRNA processing/export and protein ubiquitination. Microb Cell *11*, 69-78.
844 10.15698/mic2024.02.816.
845 61. Lim, C.S., Weinstein, B.N., Roy, S.W., and Brown, C.M. (2021). Analysis of Fungal Genomes Reveals
846 Commonalities of Intron Gain or Loss and Functions in Intron-Poor Species. Mol Biol Evol *38*, 4166-
847 4186. 10.1093/molbev/msab094.
848 62. Carmody, S.R., Tran, E.J., Apponi, L.H., Corbett, A.H., and Wente, S.R. (2010). The mitogen-activated
849 protein kinase Slt2 regulates nuclear retention of non-heat shock mRNAs during heat shock-induced
850 stress. Mol Cell Biol *30*, 5168-5179. 10.1128/MCB.00735-10.
851 63. Yona, A.H., Manor, Y.S., Herbst, R.H., Romano, G.H., Mitchell, A., Kupiec, M., Pilpel, Y., and Dahan, O.
852 (2012). Chromosomal duplication is a transient evolutionary solution to stress. Proc Natl Acad Sci U S A
853 *109*, 21010-21015. 10.1073/pnas.1211150109.
854 64. Chen, G., Bradford, W.D., Seidel, C.W., and Li, R. (2012). Hsp90 stress potentiates rapid cellular
855 adaptation through induction of aneuploidy. Nature *482*, 246-250. 10.1038/nature10795.
856 65. Shen, L., Wang, Y.T., Tang, X.X., Zhang, K., Wang, P.M., Sui, Y., and Zheng, D.Q. (2020). Heat shock
857 drives genomic instability and phenotypic variations in yeast. AMB Express *10*, 146. 10.1186/s13568-
858 020-01091-7.
859 66. Gilchrist, C., and Stelkens, R. (2019). Aneuploidy in yeast: Segregation error or adaptation mechanism?
860 Yeast *36*, 525-539. 10.1002/yea.3427.
861 67. Malik, S.C., Lin, J.D., Ziegler-Waldkirch, S., Tholen, S., Deshpande, S.S., Schwabenland, M., Schilling,
862 O., Vlachos, A., Meyer-Luehmann, M., and Schachtrup, C. (2023). Tpr Misregulation in Hippocampal
863 Neural Stem Cells in Mouse Models of Alzheimer's Disease. Cells *12*. 10.3390/cells12232757.
864 68. Mariotti, M., Kerepesi, C., Oliveros, W., Mele, M., and Gladyshev, V.N. (2022). Deterioration of the
865 human transcriptome with age due to increasing intron retention and spurious splicing. bioRxiv,
866 2022.2003.2014.484341. 10.1101/2022.03.14.484341.
867 69. Adusumalli, S., Ngian, Z.K., Lin, W.Q., Benoukraf, T., and Ong, C.T. (2019). Increased intron retention is
868 a post-transcriptional signature associated with progressive aging and Alzheimer's disease. Aging Cell
869 *18*, e12928. 10.1111/acel.12928.
870 70. Huang, W., Kew, C., Fernandes, S.A., Lohrke, A., Han, L., Demetriades, C., and Antebi, A. (2022).
871 Decreased spliceosome fidelity and egl-8 intron retention inhibit mTORC1 signaling to promote
872 longevity. Nat Aging *2*, 796-808. 10.1038/s43587-022-00275-z.

873 71. Funk, L., Su, K.C., Ly, J., Feldman, D., Singh, A., Moodie, B., Blainey, P.C., and Cheeseman, I.M.
874 (2022). The phenotypic landscape of essential human genes. Cell *185*, 4634-4653 e4622.
875 10.1016/j.cell.2022.10.017.
876 72. Janke, C., Magiera, M.M., Rathfelder, N., Taxis, C., Reber, S., Maekawa, H., Moreno-Borchart, A.,
877 Doenges, G., Schwob, E., Schiebel, E., and Knop, M. (2004). A versatile toolbox for PCR-based tagging
878 of yeast genes: new fluorescent proteins, more markers and promoter substitution cassettes. Yeast *21*,
879 947-962. 10.1002/yea.1142.
880 73. Parenteau, J., Durand, M., Veronneau, S., Lacombe, A.A., Morin, G., Guerin, V., Cecez, B., Gervais-
881 Bird, J., Koh, C.S., Brunelle, D., et al. (2008). Deletion of many yeast introns reveals a minority of genes
882 that require splicing for function. Mol Biol Cell *19*, 1932-1941. 10.1091/mbc.e07-12-1254.
883 74. Vas, A.C., Andrews, C.A., Kirkland Matesky, K., and Clarke, D.J. (2007). In vivo analysis of chromosome
884 condensation in Saccharomyces cerevisiae. Mol Biol Cell *18*, 557-568. 10.1091/mbc.e06-05-0454.
885 75. Houser, J.R., Ford, E., Chatterjea, S.M., Maleri, S., Elston, T.C., and Errede, B. (2012). An improved
886 short-lived fluorescent protein transcriptional reporter for Saccharomyces cerevisiae. Yeast *29*, 519-530.
887 10.1002/yea.2932.
888 76. Edelstein, A.D., Tsuchida, M.A., Amodaj, N., Pinkard, H., Vale, R.D., and Stuurman, N. (2014).
889 Advanced methods of microscope control using muManager software. J Biol Methods *1*.
890 10.14440/jbm.2014.36.
891 77. Rahman, S., and Zenklusen, D. (2013). Single-molecule resolution fluorescent in situ hybridization
892 (smFISH) in the yeast S. cerevisiae. Methods Mol Biol *1042*, 33-46. 10.1007/978-1-62703-526-2_3.

893

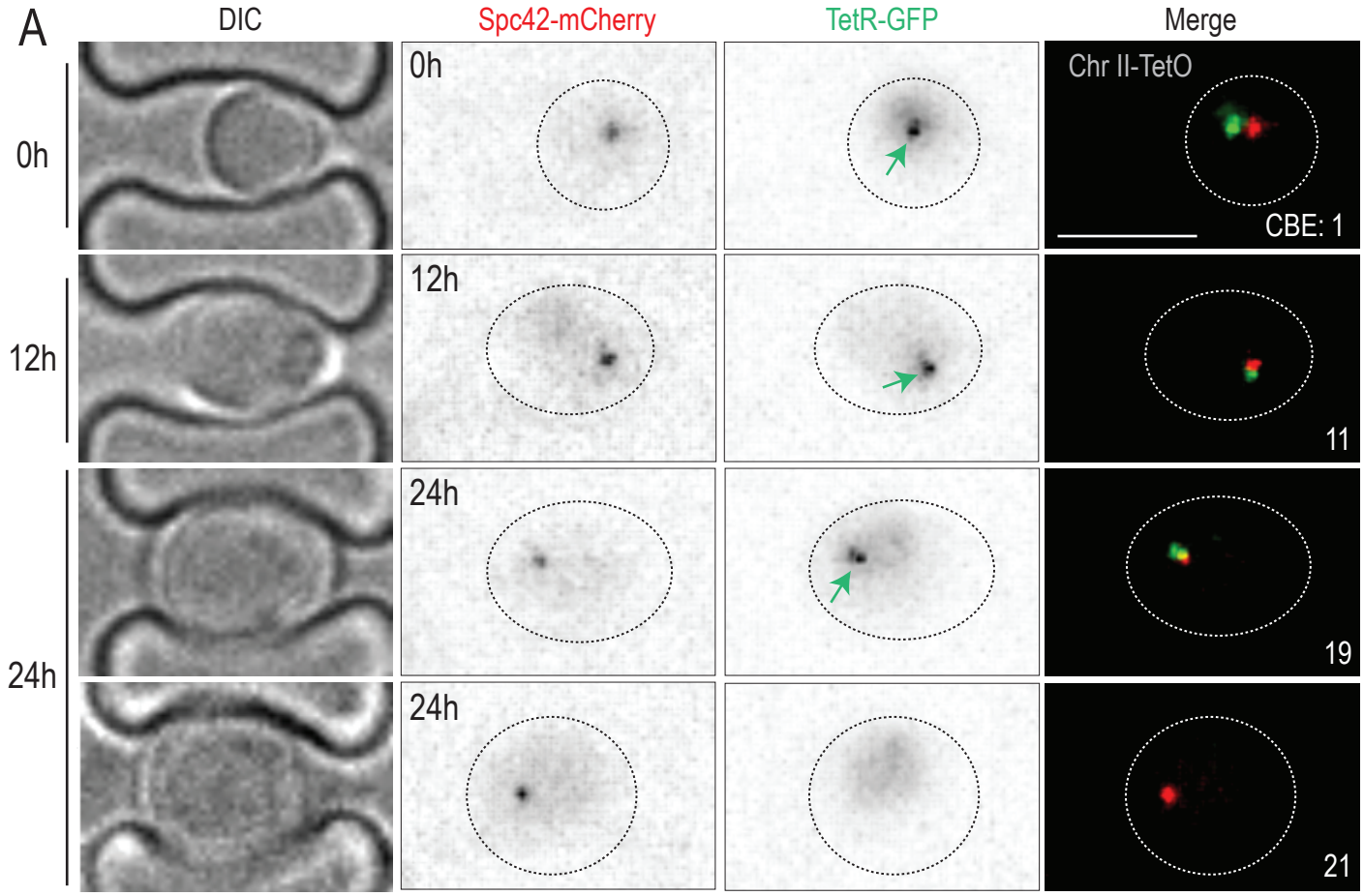
A
DIC
Spc42-mCherry
TetR-GFP
Merge
0h
12h
24h
Chr II-TetO
CBE: 1
11
19
21

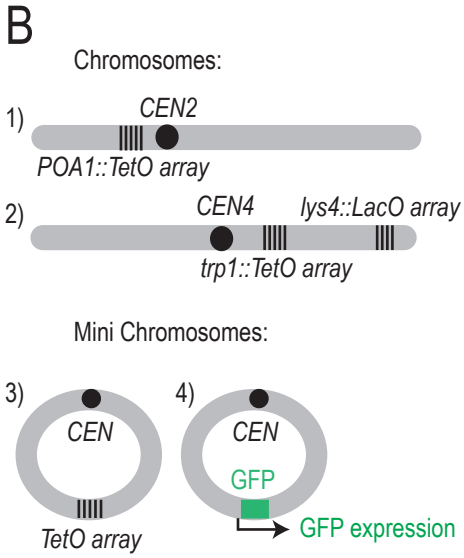
B
Chromosomes:
1)
CEN2
POA1::TetO array
2)
CEN4
lys4::LacO array
trp1::TetO array
Mini Chromosomes:
3)
CEN
TetO array
4)
CEN
GFP
GFP expression

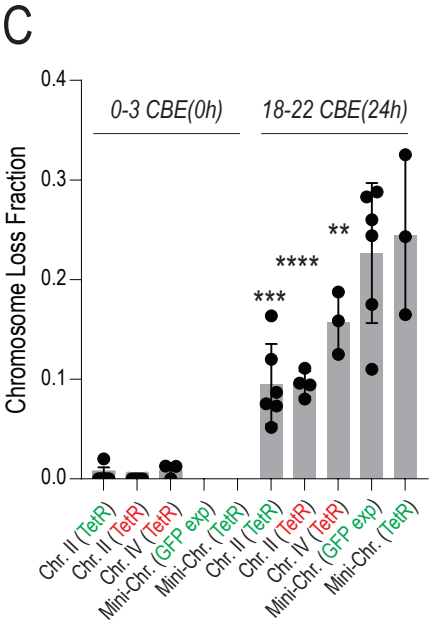
C
Chromosome Loss Fraction
0-3 CBE(0h)
18-22 CBE(24h)
0.4
0.3
0.2
0.1
0.0
***
****
**
Chr. II (TetR)
Chr. II (TetR)
Chr. IV (TetR)
Mini-Chr. (GFP exp)
Mini-Chr. (TetR)
Chr. II (TetR)
Chr. II (TetR)
Chr. IV (TetR)
Mini-Chr. (GFP exp)
Mini-Chr. (TetR)

Figure 1

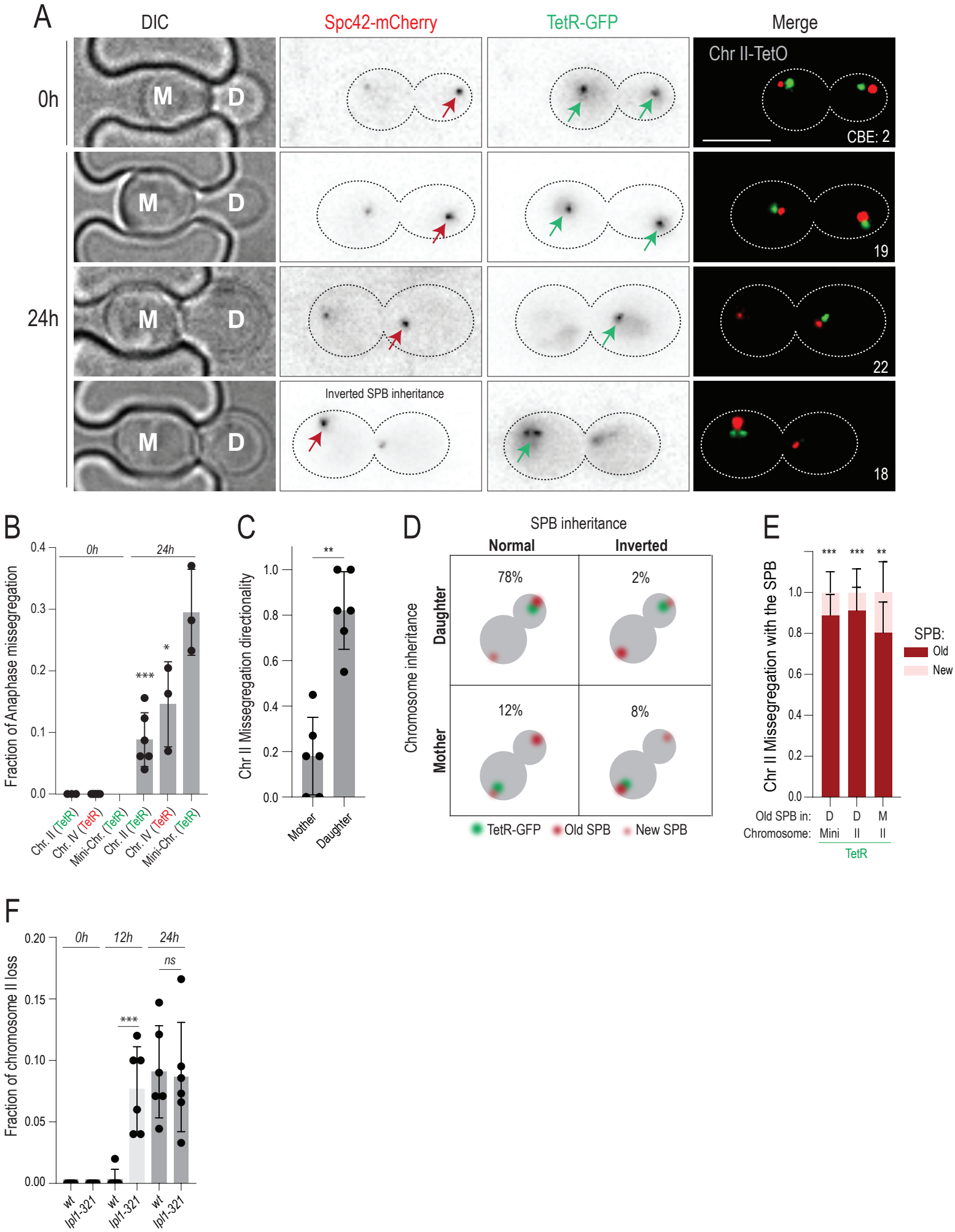
A
DIC
Spc42-mCherry
TetR-GFP
Merge
0h
24h
M
D
Chr II-TetO
CBE: 2
19
22
18
Inverted SPB inheritance
B
Fraction of Anaphase missegregation
0h
24h
Chr. II (TetR)
Chr. IV (TetR)
Mini-Chr. (TetR)
C
Chr II Missegregation directionality
Mother
Daughter
D
SPB inheritance
Normal
Inverted
Chromosome inheritance
Daughter
Mother
78%
2%
12%
8%
TetR-GFP
Old SPB
New SPB
E
Chr II Missegregation with the SPB
SPB:
Old
New
Old SPB in:
Chromosome:
TetR
F
Fraction of chromosome II loss
0h
12h
24h
ns
wt
lpl1-321

Figure 2

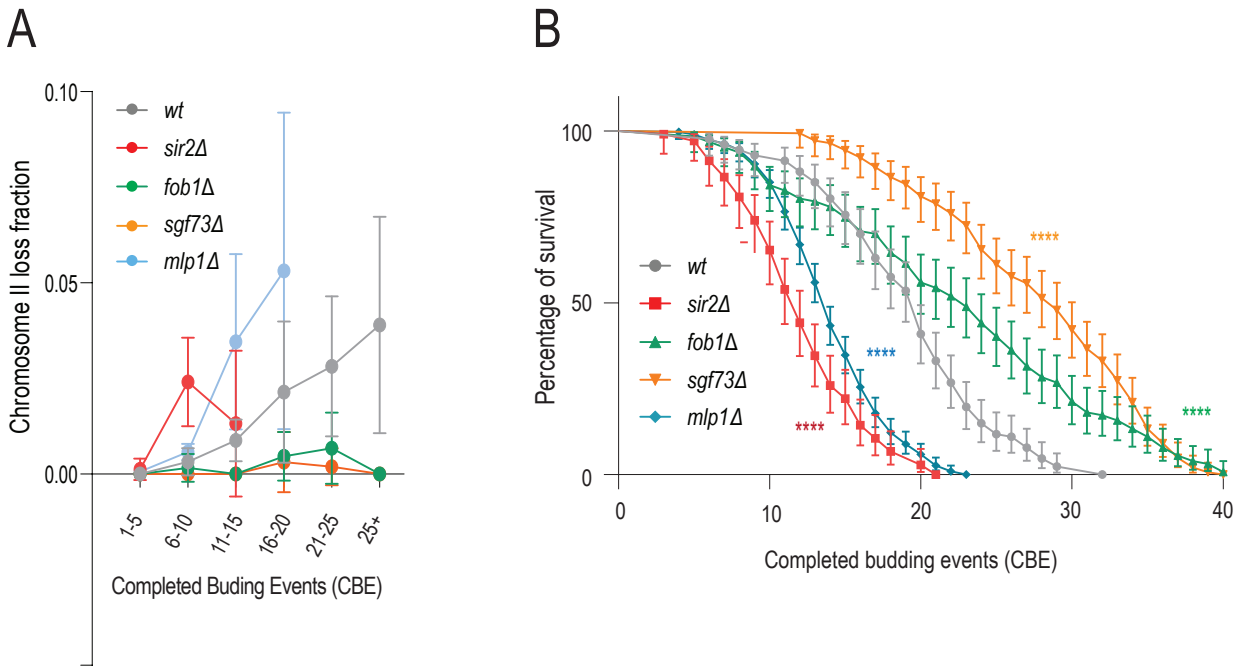
A
0.10
0.05
0.00
Chromosome II loss fraction
wt
sir2Δ
fob1Δ
sgf73Δ
mlp1Δ
1-5
6-10
11-15
16-20
21-25
25+
Completed Buding Events (CBE)
B
100
50
0
Percentage of survival
wt
sir2Δ
fob1Δ
sgf73Δ
mlp1Δ
****
****
****
****
0
10
20
30
40
Completed budding events (CBE)

Figure 3

A

Yeast genes encoding kinetochore-associated proteins

CBF3	NDC10	CCAN	MIF2	CPC	IPL1	SAC	MAD1
	CEP3		CSE4		SLI15		MAD2
	CTF13		CTF19		NBL1		BUB1
	SKP1		OKP1		BIR1		BUB3
			MCM21				MPS1
CBF1			AME1	SPC105	SPC105	Motor	KIP1
			CHL4		YDR532		KIP3
			CNN1				CIN8
MIS12	MTW1		WIP1	DAM1	ASK1		KAR3
	DSN1		MHF1		DAD1	MAPS	SLK19
	NNF1		MHF2		DAD2		BIK1
	NSL1		MCM16		DAD3	Phosphatase	GLC7
			CTF3		DAD4		CDC14
NDC80	NDC80		MCM22		DAM1		
	NUF2		IML3/MCM19		DUO1		
	SPC24		NKP1		SPC19		
	SPC25		NKP2		SPC34		
			YBP2		HSK1		

Adapted from:
Biggins et al 2013

B

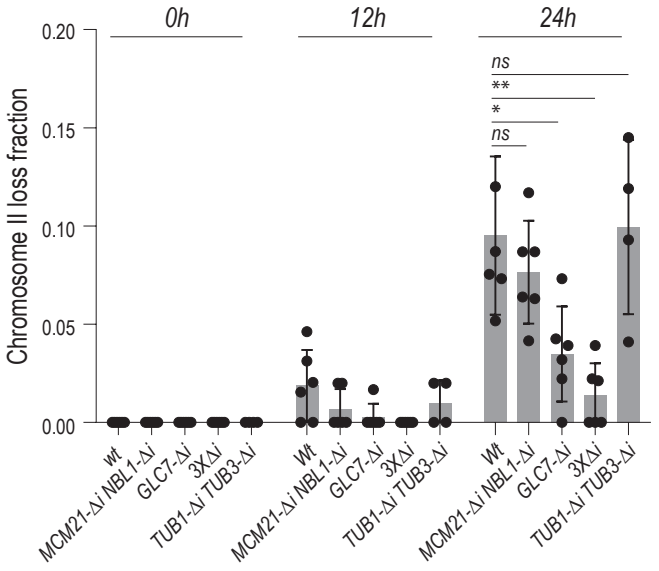

C

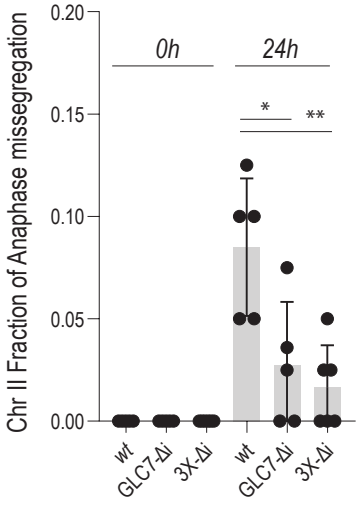

D

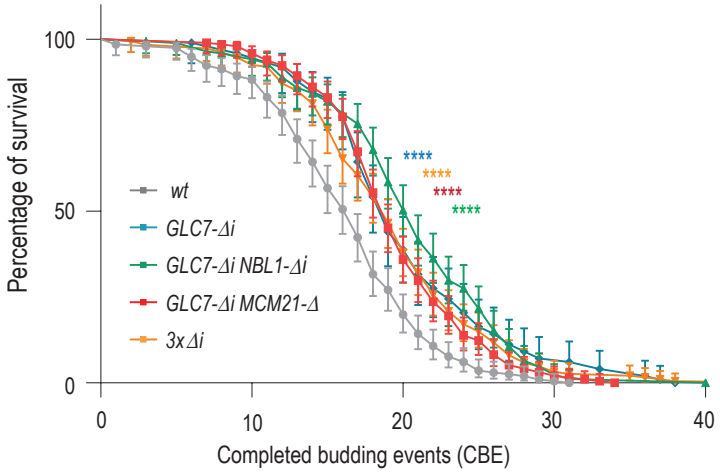

Figure 4

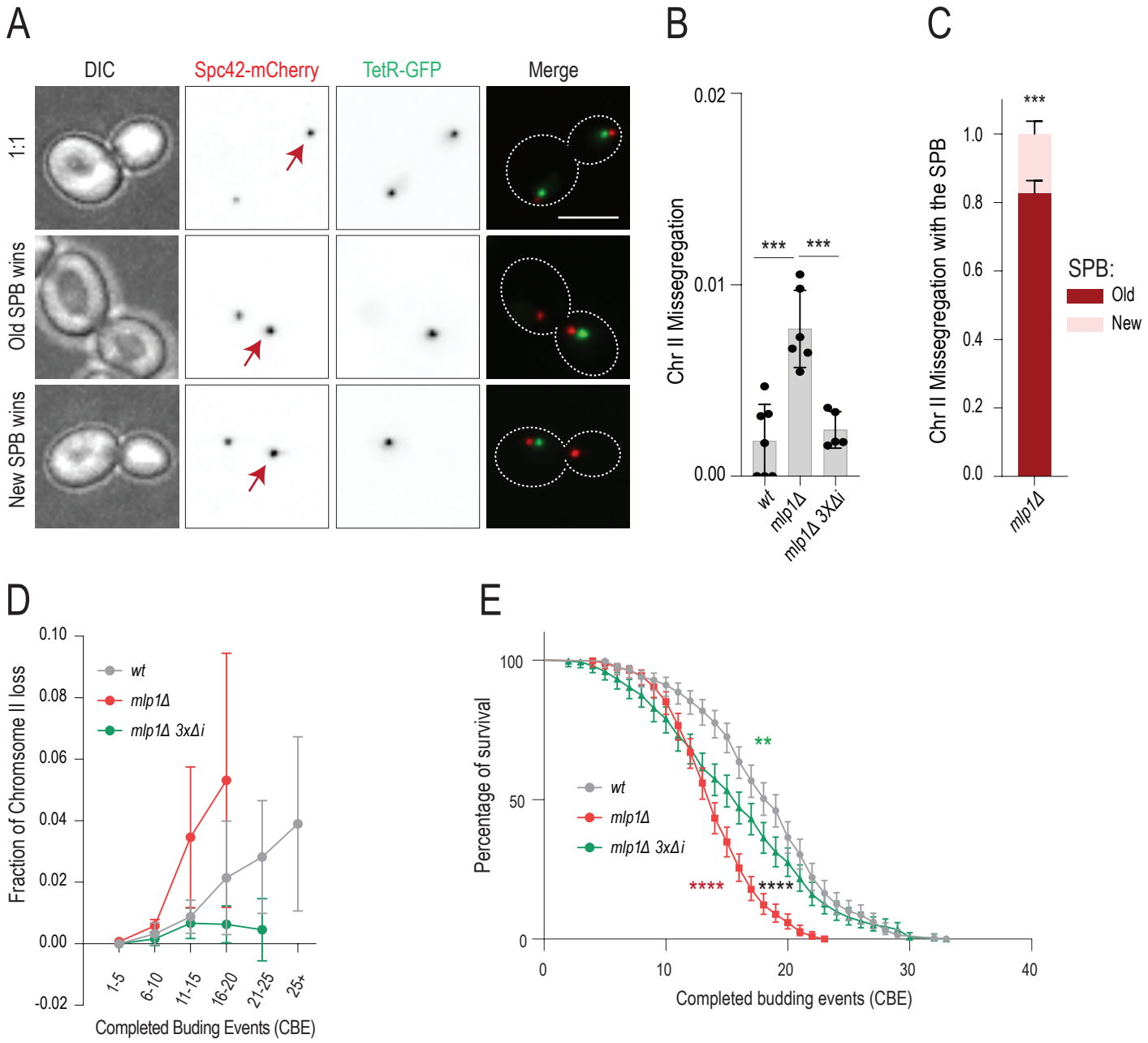
A
DIC
Spc42-mCherry
TetR-GFP
Merge
1:1
Old SPB wins
New SPB wins
B
Chr II Missegregation
0.02
0.01
0.00
***
***
wt
mlp1Δ
mlp1Δ 3XΔi
C
Chr II Missegregation with the SPB
1.0
0.8
0.6
0.4
0.2
0.0
***
SPB:
Old
New
mlp1Δ
D
Fraction of Chromsome II loss
0.10
0.08
0.06
0.04
0.02
0.00
-0.02
wt
mlp1Δ
mlp1Δ 3xΔi
1-5
6-10
11-15
16-20
21-25
25+
Completed Buding Events (CBE)
E
Percentage of survival
100
50
0
wt
mlp1Δ
mlp1Δ 3xΔi
**
****
****
0
10
20
30
40
Completed budding events (CBE)

Figure 5

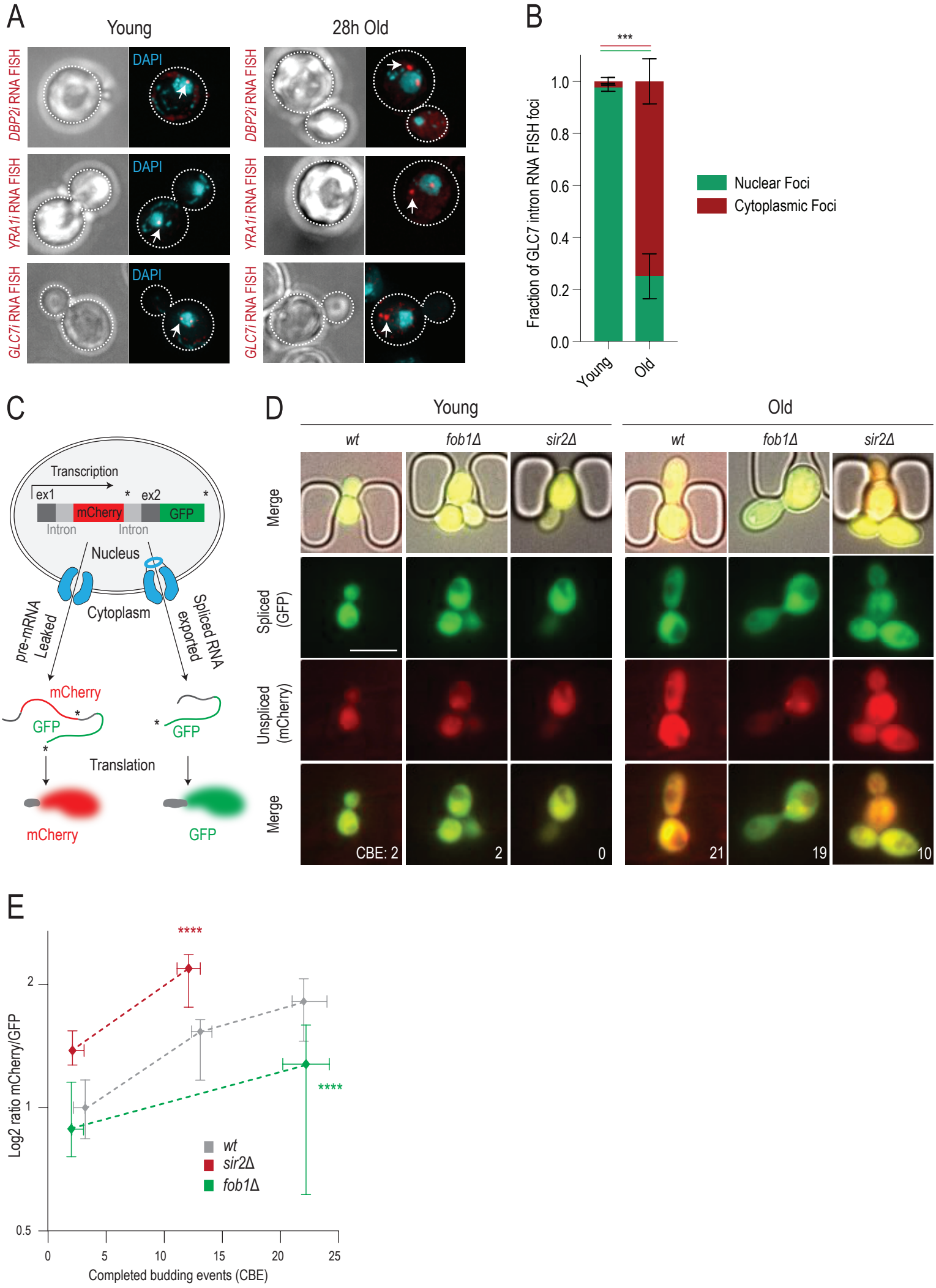
A
Young
28h Old
DBP2i RNA FISH
YRA1i RNA FISH
GLC7i RNA FISH
DAPI
B
***
Fraction of GLC7 intron RNA FISH foci
1.0
0.8
0.6
0.4
0.2
0.0
Young
Old
Nuclear Foci
Cytoplasmic Foci
C
Transcription
ex1
ex2
mCherry
GFP
Intron
Intron
Nucleus
Cytoplasm
pre-mRNA Leaked
Spliced RNA exported
mCherry
GFP
GFP
Translation
mCherry
GFP
D
Young
Old
wt
fob1Δ
sir2Δ
wt
fob1Δ
sir2Δ
Merge
Spliced (GFP)
Unspliced (mCherry)
Merge
CBE: 2
2
0
21
19
10
E
****
****
Log2 ratio mCherry/GFP
2
1
0.5
0
5
10
15
20
25
Completed budding events (CBE)
wt
sir2Δ
fob1Δ

Figure 6

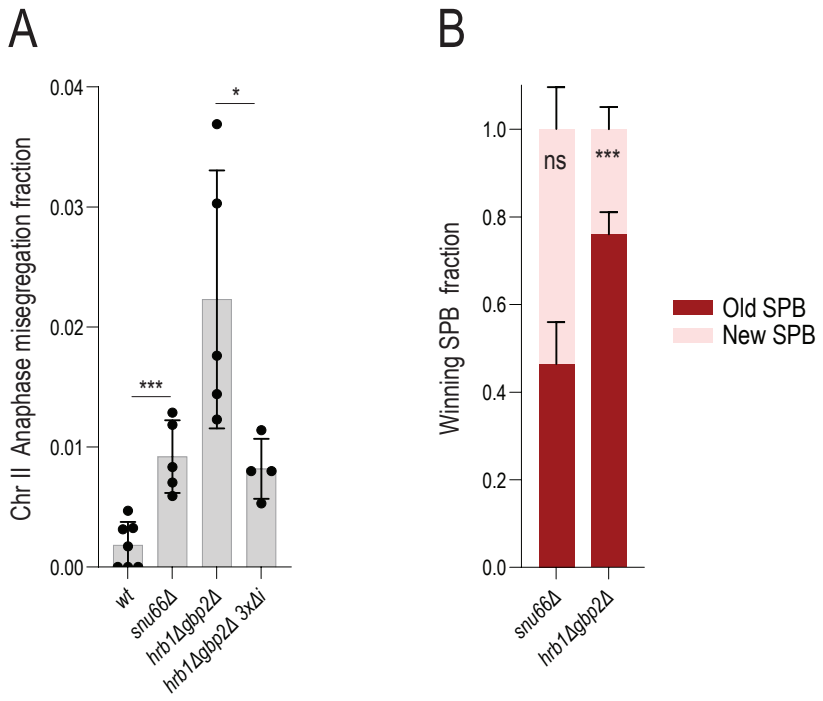
A
Chr II Anaphase misegregation fraction
0.04
0.03
0.02
0.01
0.00
***
*
wt
snu66Δ
hrb1Δgbp2Δ
hrb1Δgbp2Δ 3xΔi
B
Winning SPB fraction
1.0
0.8
0.6
0.4
0.2
0.0
ns
***
snu66Δ
hrb1Δgbp2Δ
Old SPB
New SPB

Figure 7

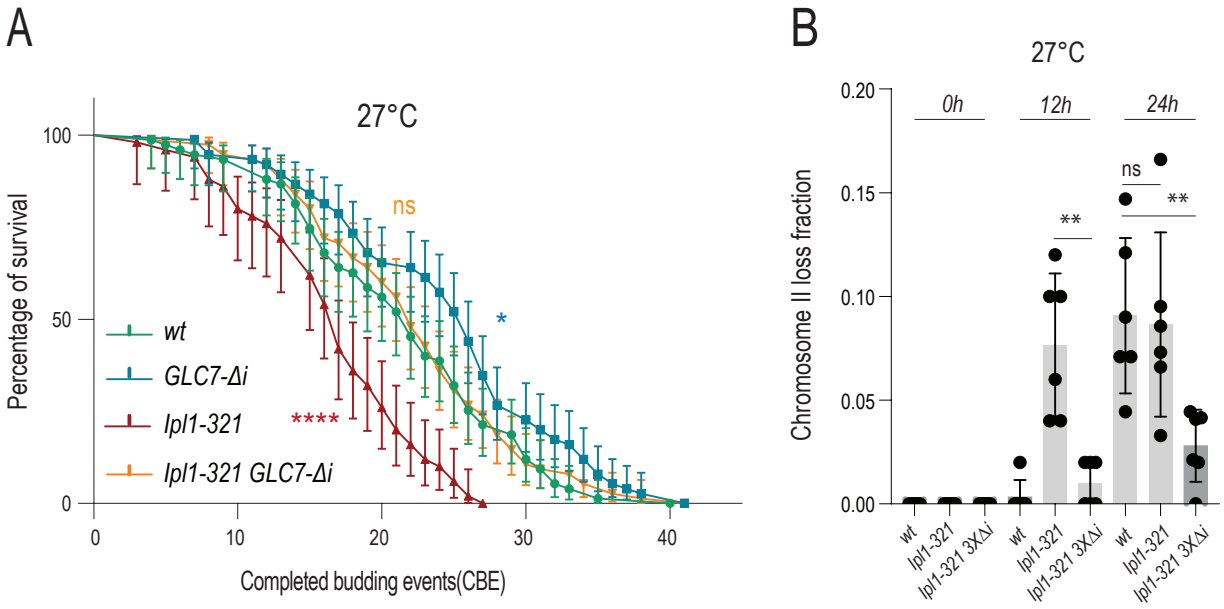

Supplementary Fig 1

A

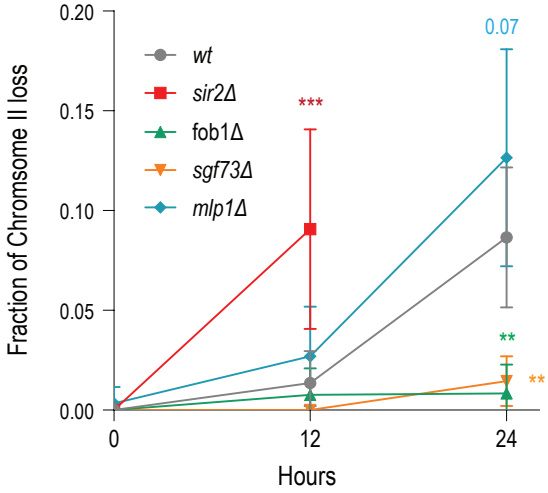

Supplementary Fig 2

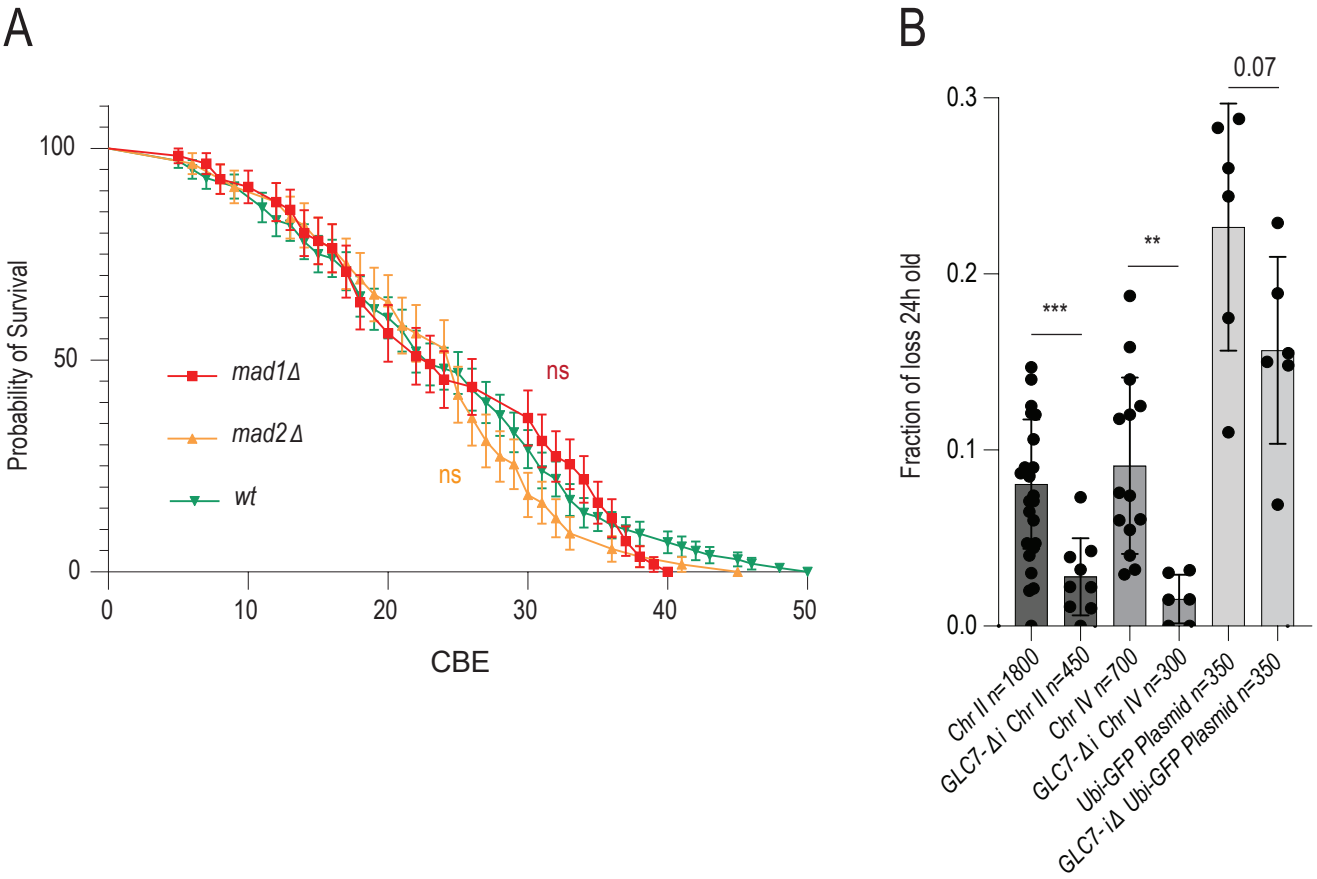

Supplementary Fig 3

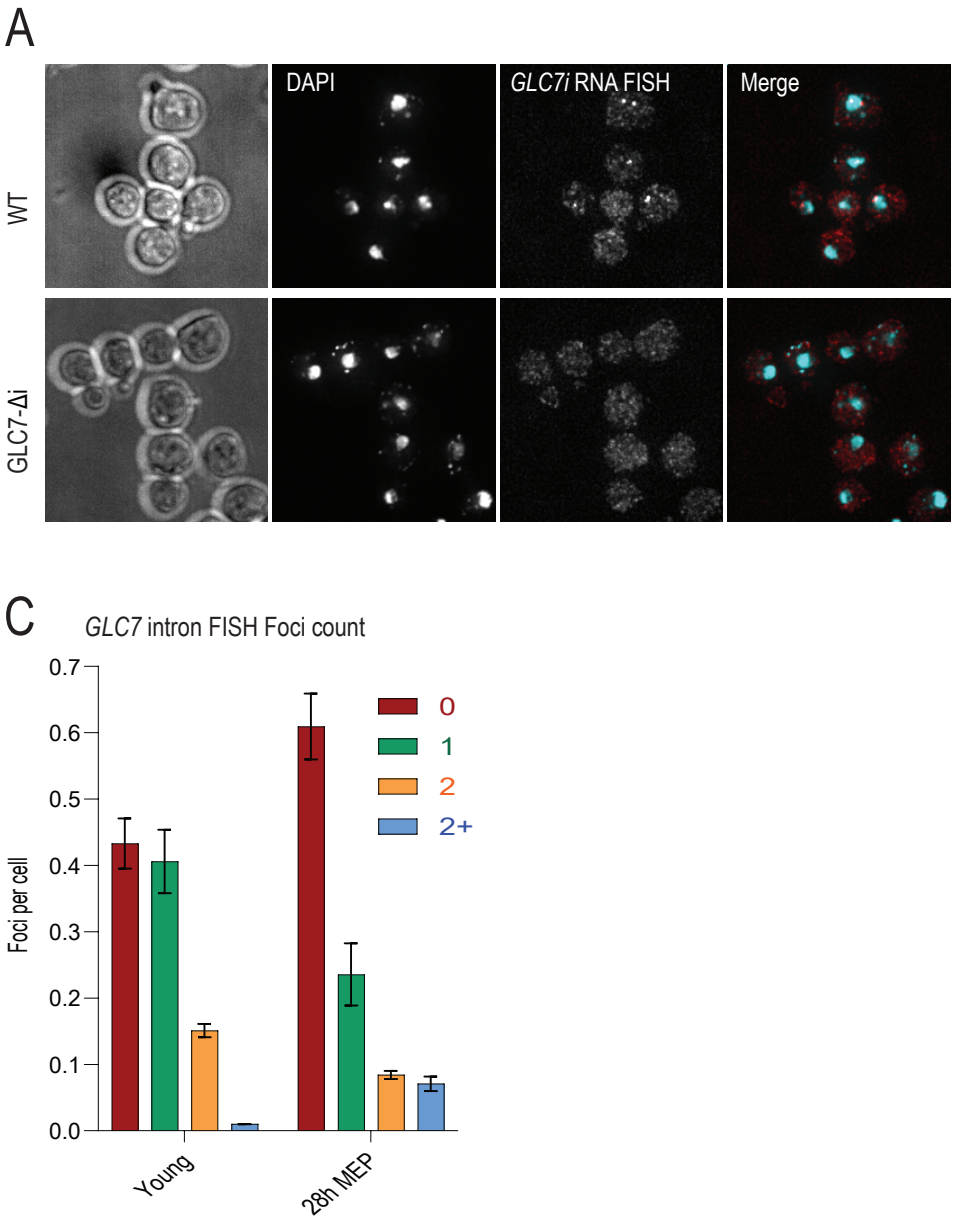

Supplementary Fig 4